Title
Nanodisk: a versatile drug delivery platform

Author
Ghosh, Mistuni

Publication Date
2012

Peer reviewed|Thesis/dissertation

NANODISK: A VERSATILE DRUG DELIVERY PLATFORM

By

Mistuni Ghosh

A dissertation submitted in partial satisfaction of the

requirements for the degree of

Doctor of Philosophy

in

Metabolic Biology

in the

Graduate Division

of the

University of California, Berkeley

Committee in charge:

Professor Robert O. Ryan, Co-chair
Professor Jen-Chywan (Wally) Wang, Co-chair
Professor Barry Shane
Professor Amy E. Herr

Fall 2012

ABSTRACT

NANODISK: A VERSATILE DRUG DELIVERY PLATFORM

by

Mistuni Ghosh

Doctor of Philosophy in Metabolic Biology

University of California, Berkeley

Professor Robert O. Ryan, Co-Chair

Professor Jen-Chywan (Wally) Wang, Co-Chair

According to the definition from the National Nanotechnology Initiative, nanotechnology refers to research conducted at a nano-scale level which is about 1 to 100 nanometers (nm). Recent years have seen widespread application of nanotechnology in the field of drug delivery. Using nanotechnology, it is possible to package drugs at a nano-scale level to improve bioavailability, increase plasma circulation time and achieve tissue specific drug delivery with concomitant reduction in possible adverse side effects.

Nanodisks (ND) are self assembled nanoparticles comprised of a phospholipid bilayer stabilized by an apolipoprotein "scaffold". ND can be formulated with significant amounts of bioactive agents. The ND architecture is reminiscent of nascent high density lipoprotein (HDL) particles. In the physiological context, nascent HDL picks up excess cholesterol from peripheral tissues and transports it to the liver for excretion or re-use. *In vitro*, nascent HDL particles can be reconstituted by incubating phospholipid vesicles with apolipoprotein molecules. In reconstituted HDL (rHDL) the phospholipids arrange as a disk-shaped bilayer with two or more apolipoprotein molecules circumscribing the edge of the disk. In recent years rHDL have emerged as a platform for incorporation and transport of hydrophobic and amphipathic biomolecules. To distinguish rHDL loaded with a bioactive agent from physiological HDL we have coined the terminology ND. The focus of my research has been to evaluate ND's ability to function as a vehicle for two different bioactive agents- curcumin, a polyphenol with anti-cancer properties and small interfering RNA (siRNA), novel nucleic acid molecules with enormous therapeutic potential.

Curcumin is water insoluble and oral administration results in poor systemic bioavailability. Hence, the development of a suitable intravenous delivery vehicle is crucial for curcumin's clinical success. Incorporation of curcumin into ND generates a water soluble formulation suitable for intravenous delivery. Compared to free curcumin,

curcumin-ND displayed improved cellular uptake of curcumin, which translated into potent biological effects in established tumor cell lines. Strategic use of an apolipoprotein scaffold, known to bind receptors over-expressed on certain tumor cells, caused further improvement in ND mediated curcumin delivery. In other studies, synthetic siRNA mediated silencing of validated disease targets has been shown to improve clinical outcomes in relevant disease models. However, successful therapeutic application of siRNA relies upon the development of a carrier that protects the siRNA molecules from serum nucleases and facilitates their efficient delivery to target tissues, minimizing off-target effects. In my studies I show that an optimum mole percent of a bilayer forming cationic lipid can be included in the ND formulation generating intact nanometer sized positively charged ND (i.e. cationic lipid ND). Cationic lipid ND stably bound 23-mer double stranded oligonucleotides and experiments showed that cationic lipid ND-bound siRNA efficiently knocked down a target gene in hepatocarcinoma cells. Results indicate that cationic lipid ND have the potential to function as a siRNA carrier.

As a delivery vehicle ND possess several advantages. ND components are biocompatible and their assembly is facile. The potential to engineer the apolipoprotein scaffold, in addition to interchangeability of the lipid and scaffold components, makes ND a versatile delivery platform.

ACKNOWLEDGEMENTS

I would like to thank my husband for his unwavering support through the years I pursued my graduate studies. His support encouraged me to dream big and his confidence in my abilities made me set high goals for myself. Debabrata, I could not have done this without you.

I would also like to thank my parents for teaching me to be respectful, work hard and have a positive outlook even in the face of adversity.

I would like to take this opportunity to thank Bob, my mentor, for his support, guidance and encouragement which motivated me to work hard, take initiative and think out of the box.

Finally, I would like to acknowledge my sons, Purajit and Ronobir, for being patient through this whole process and making my job as a mom easier.

TABLE OF CONTENTS

LIST OF TABLES

LIST OF FIGURES

CHAPTER 1:
INTRODUCTION

1.1. Abbreviations

apo = apolipoprotein
DMPC = 1,2-dimyristoyl-*sn*-glycero-3-phosphocholine
DMTAP = 1,2-dimyristoyl-3-trimethylammonium-propane
ND = nanodisk
rHDL = reconstituted high-density lipoprotein
RNAi = RNA interference
siRNA = short interfering RNA

Inexpensive and straightforward assembly, biocompatibility and tissue targeting capability are some of the hallmarks for an ideal drug delivery vehicle. Nanodisks (ND) are self assembled biocompatible lipid-protein nanoparticles that can function as a drug carrier. ND are composed of commercially available synthetic phospholipids and recombinant apolipoprotein. Presentation of apolipoprotein molecules to pre-formed phospholipid vesicles transforms the vesicles to discoidal nano-sized ND with the apolipoprotein molecules functioning as a stabilizing scaffold. ND's ability to function as an efficient delivery vehicle is demonstrated with the bioactive polyphenol curcumin. Curcumin, a natural polyphenol has emerged as an anti-cancer agent but its clinical use has been hindered due to poor bioavailability following oral dosing. Solubilization of curcumin into ND generates a water soluble formulation suitable for direct systemic administration with possibly improved pharmacological outcome. The ability to easily manipulate ND composition, to suit specific drug delivery needs, makes ND a versatile delivery platform. Inclusion of bilayer forming synthetic cationic lipids in the ND formulation generates charged ND that show promise as a siRNA delivery vehicle.

1.2. Application of the nanodisk technology in drug delivery

Hydrophobicity, poor serum stability and fast metabolism/degradation along with rapid clearance are some of the properties which hinder clinical use of certain promising bioagents. Formulation of such compounds in a suitable delivery vehicle will improve bioavailability, increase plasma circulation time and result in enhanced uptake at target tissue sites with minimal off target effects (1). An ideal delivery vehicle is one that has a straightforward assembly, is biodegradable, solubilizes high amounts of the bioactive compound and can be easily tweaked at the molecular level to achieve tissue or cell type specific targeted delivery. Nanodisks (ND) are self assembled lipid/protein nano-particles that can be loaded with high amounts of pharmacologically active compounds (2). The structure and composition of ND are similar to nascent high-density lipoprotein (HDL) particles. Nascent HDL, circulating in the plasma, play a key role in the reverse cholesterol transport (RCT) pathway. It collects unesterified cholesterol from macrophages and foam cells for delivery to liver for excretion or re-use (3). During RCT discoidal nascent HDL undergo a step-wise maturation into an esterified-cholesterol-laden spherical mature HDL. In contrast to the tremendous structural and compositional complexity of mature HDL, the basic architecture of nascent HDL is quite simple, comprised of only phospholipid and apolipoprotein. In fact, when phospholipid vesicles are incubated with apolipoprotein molecules *in vitro*, the amphipathic α-helix structural motif of the apolipoprotein molecules induces transformation of the vesicles into discoidal reconstituted HDL (rHDL) particles (**Figure 1-1**). In recent years rHDL has emerged as a suitable drug delivery platform (2, 4). Drug-loaded rHDL particles are called ND to distinguish them from natural HDL of physiological origin. ND are formed by direct self assembly using synthetic phospholipid dimyristoylphosphatidylcholine (DMPC) and an apolipoprotein (apo), usually apo A-I or E. In the ND product particles DMPC molecules form a disk-shaped bilayer with their hydrophilic head groups exposed to the aqueous surrounding and their hydrocarbon chains buried in the bilayer. Two or more apolipoprotein molecules, by virtue of their intrinsic amphipathic α-helixes, wrap around the bilayer edge protecting the exposed hydrocarbon chains from the aqueous environment. Hence, apolipoprotein's secondary structure is fundamental to both the formation and integrity of ND. ND's ability to function as a delivery vehicle has been demonstrated with different hydrophobic biomolecules (5-7). The modular lipid-protein assembly of ND is amenable to manipulations at the molecular level. Cargo-specific customization is possible by titrating variety of lipids into the ND vehicle. All members of the apolipoprotein family possess the characteristic amphipathic helixes and have the ability to transform phospholipid vesicles into ND. They can be used interchangeably to function not only as a stabilizing scaffold but also as a ND component that mediates direct physical interaction with specific cell types. Furthermore, the apolipoprotein scaffold can be modified by protein engineering (8), expanding the repertoire of cell types that can be targeted by ND. Straightforward assembly, ability to carry high amounts of bioactive compounds and biocompatible lipid-protein components that can be tuned at the molecular level makes ND a promising nano-platform for *in vivo* drug delivery applications.

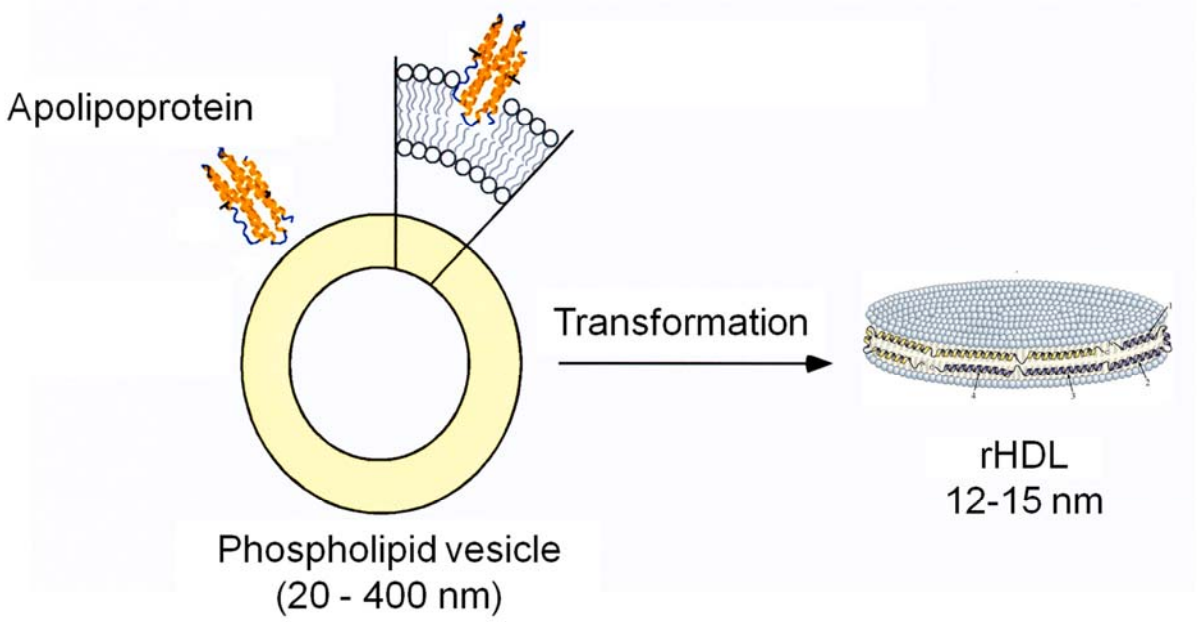

Figure 1-1. Formation of rHDL. Apolipoprotein molecules mediate transformation of phospholipid vesicle to rHDL. In the product rHDL particle two or more apolipoprotein molecules wrap around the bilayer edge shielding the hydrocarbon chains from the aqueous environment (not drawn to scale).

1.3. Nanodisk: a delivery vehicle for the polyphenol curcumin

Curcumin (diferuloylmethane) is a hydrophobic polyphenol derived from rhizome of the herb *Curcuma longa*. Accumulating preclinical data suggests that curcumin possesses several beneficial properties including anti-inflammatory, anti-oxidant and anti-proliferative activities (9-13). The pleiotropic effects of curcumin stem from its' ability to influence multiple signaling pathways, many of which are dysregulated in cancer cells. Furthermore, curcumin is non-toxic, even at relatively high doses (14). Despite this, clinical advancement of this promising molecule has suffered due to its poor water solubility, short biological half-life, and low bioavailability following oral administration (15, 16). Attempts to overcome these limitations have led to the synthesis of curcumin analogues (17), use of adjuvants as well as development of improved delivery platforms such as liposomes and nanoparticles (18-21).

Incorporation of curcumin into ND overcomes the poor water solubility of this bioactive phytochemical (7). The particles generated are nanoscale, disk-shaped complexes of curcumin, DMPC and apoA-I. **Figure 1-2** shows the curcumin-ND formulation scheme. Compared to free curcumin, curcumin-ND induced potent anti-proliferative and apoptotic effects in established mammalian tumor cell lines (7, 22). ND with apoE as the scaffold further enhanced curcumin uptake in brain tumor cells expressing high amounts of cell surface proteins that specifically interact with apoE. Enhanced uptake translated into potent cytotoxic and apoptotic effects. ND's ability to solubilize curcumin with complete retention of its biological effects along with the possibility of using the ND scaffold for enhanced intracellular curcumin delivery indicates that the nano-sized biocompatible ND platform may be a suitable systemic delivery vehicle for curcumin.

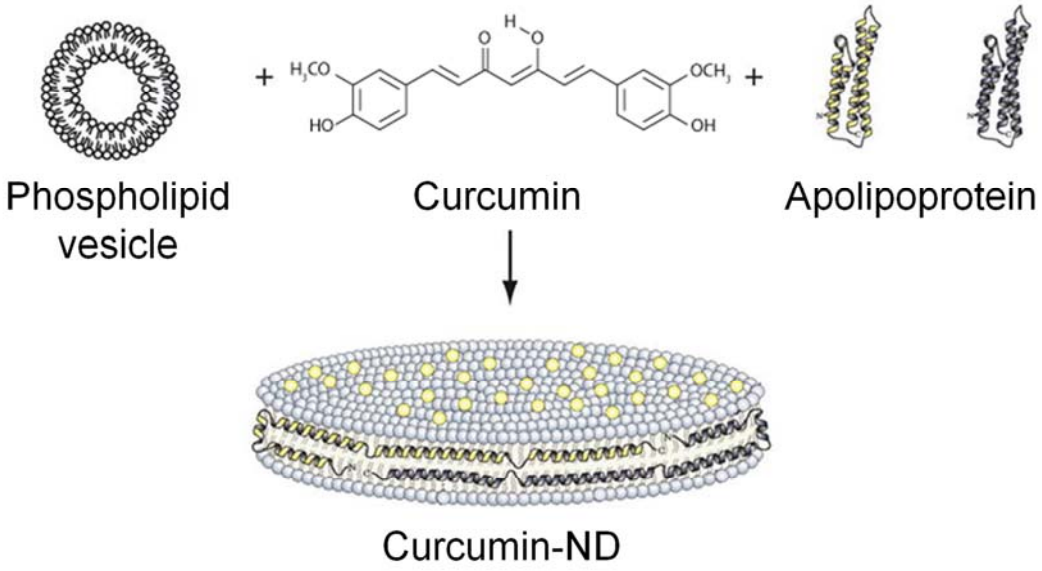

Figure 1-2. Curcumin-ND formulation scheme. Yellow dots on curcumin-ND represent curcumin molecules.

1.4. Cationic Lipid nanodisk

Small interfering RNA (siRNA), also called short interfering RNA, is a class of bioactive macromolecules that engages the endogenous RNA interference (RNAi) pathway to silence disease causing genes. siRNA mediated silencing of validated disease targets have been shown to improve clinical outcome in relevant disease models (23-26). However, low serum stability and the need for precise intracellular delivery of the siRNA molecules have prevented its widespread clinical application. This has led to the development of several siRNA delivery strategies (27-32) including cationic lipid based delivery platforms (33-35). ND are lipid-protein particles that can be manipulated at the molecular level. Titration of different lipids in the ND formulation generates intact nanoparticles. When thirty percent of the neutral phospholipid DMPC in the ND formulation was replaced with the synthetic cationic lipid dimyristoyltrimethylammonium propane (DMTAP), intact nanoparticles were formed. **Figure 1-3** shows the chemical structure of DMPC and DMTAP. The bilayer forming DMTAP molecules insert into ND with their positively charged head group exposed for interaction with siRNA molecules. The positively charged ND thus formed are referred to as cationic lipid ND. *In vitro*, the cationic lipid ND bound stably with synthetic nucleic acid molecules that mimic siRNA and cationic lipid ND-bound GAPDH siRNA caused efficient GAPDH knock down in cultured hepatoma cells. Studies conducted thus far indicate that cationic lipid ND have the potential to function as a siRNA carrier.

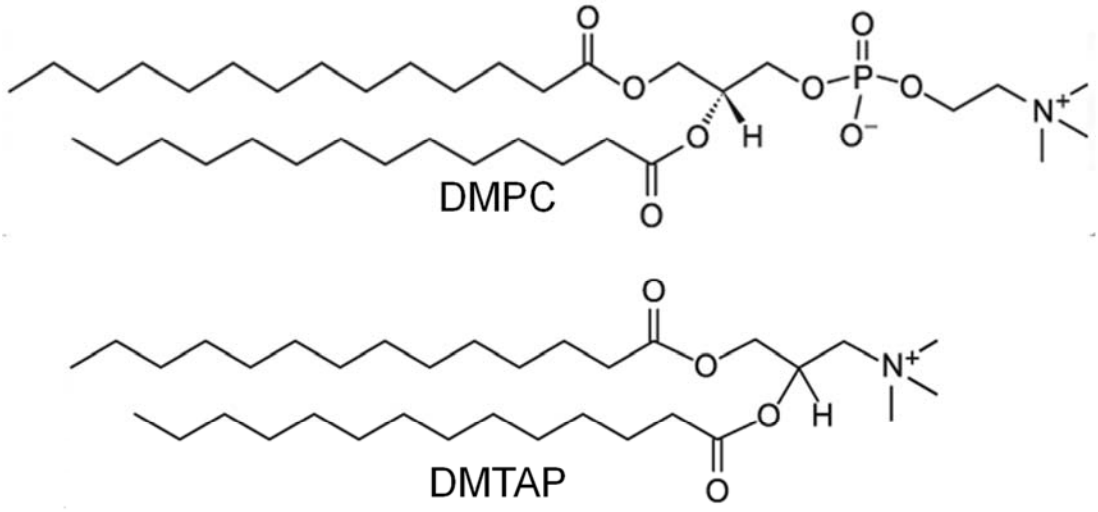

Figure 1-3. Chemical structures of DMPC and DMTAP.

1.5. References

(1) Farokhzad OC, Langer R. Impact of nanotechnology on drug delivery. ACS Nano. 2009; 3:16-20.
(2) Ryan RO. Nanobiotechnology applications of reconstituted high density lipoprotein. J Nanobiotechnology. 2010; 8:28.
(3) Brewer HB Jr. Clinical review: The evolving role of HDL in the treatment of high-risk patients with cardiovascular disease. J Clin Endocrinol Metab. 2011; 96:1246-1257.
(4) Bricarello DA, Smilowitz JT, Zivkovic AM, German JB, Parikh AN. Reconstituted lipoprotein: a versatile class of biologically-inspired nanostructures. ACS Nano. 2011; 5:42-57.
(5) Oda MN, Hargreaves PL, Beckstead JA, Redmond KA, van Antwerpen R, Ryan RO. Reconstituted high-density lipoprotein enriched with the polyene antibiotic, amphotericin B. J Lipid Res 2006; 47:260-267.
(6) Redmond KA, Nguyen TS, Ryan RO. All-trans retinoic acid nanodisks. Int J Pharm 2007; 339:246-250.
(7) Ghosh M, Singh ATK, Xu W, Sulchek T, Gordon LI, Ryan RO. Curcumin nanodisks: formulation and characterization. Nanomedicine 2011; 7:162-167.
(8) Iovannisci DM, Beckstead JA, Ryan RO. Targeting nanodisks via a single chain variable antibody--apolipoprotein chimera. Biochem Biophys Res Commun. 2009; 379:466-469.
(9) Jurenka JS. Anti-inflammatory properties of curcumin, a major constituent of Curcuma longa: a review of preclinical and clinical research. Alternative Medicine Review 2009; 14:141-153.
(10) Epstein J, Sanderson IR, Macdonald TT. X. Curcumin as a therapeutic agent: the evidence from in vitro, animal and human studies. Br J Nutr 1994; 26:1-13.
(11) Kunnumakkara AB, Anand P, Aggarwal BB. Curcumin inhibits proliferation, invasion, angiogenesis and metastasis of different cancers through interaction with multiple cell signaling proteins. Cancer Letters 2008; 269:199-225.
(12) Hatcher H, Planalp R, Cho J, Torti FM, Torti SV. Curcumin: from ancient medicine to current clinical trials. Cell Mol Life Sci 2008; 65:1631-1652.
(13) Gupta SC, Prasad S, Kim JH, Patchva S, Webb LJ, Priyadarsini IK, Aggarwal BB. Multitargeting by curcumin as revealed by molecular interaction studies. Nat Prod Rep. 2011; 28:1937-55.
(14) Strimpakos AS, Sharma RA. Curcumin: preventive and therapeutic properties in laboratory studies and clinical trials. Antioxidants and Redox Signaling 2008; 10:511-545.
(15) Anand P, Kunnumakkara AB, Newman RA, Aggarwal BB. Bioavailability of curcumin: problems and promises. Molecular pharmaceutics 2007; 4:807-818.
(16) Bisht, S, Maitra A. Systemic delivery of curcumin: 21st century solutions for an ancient conundrum. Curr Drug Discov Technol 2009; 6:192-199.
(17) Agrawal DN, Mishra PK. Curcumin and its analogues: potential anticancer agents. Medicinal Research Reviews 2010; 30:818-860.

(18) Bisht S, Feldmann G, Soni S, Ravi R, Karikar C, Maitra A, Maitra A. Polymeric nanoparticle-encapsulated curcumin ("nanocurcumin"): a novel strategy for human cancer therapy. Journal of Nanobiotechnology 2007; 5:3.
(19) Marczylo TH, Verschoyle RD, Cooke DN, Morazzoni P, Steward WP, Gescher AJ. Comparison of systemic availability of curcumin with that of curcumin formulated with phosphatidylcholine. Cancer Chemother Pharmacol 2007; 60:171-177.
(20) Narayanan NK, Nargi D, Randolph C, Narayanan BA. Liposome encapsulation of curcumin and resveratrol in combination reduces prostate cancer incidence in PTEN knockout mice. Int J Cancer 2009; 125:1-8.
(21) Thangapazham RL, Puri A, Tele S, Blumenthal R, Maheshwari RK. Evaluation of a nanotechnology based carrier for delivery of curcumin in prostate cancer cells. Int J Oncol 2008; 32:1119-1123.
(22) Singh ATK, Ghosh M, Forte TM, Ryan RO, Gordon LI. Curcumin nanodisk-induced apoptosis in mantle cell lymphoma. Luekemia and Lymphoma 2011; 52:1537-1543.
(23) Frank Y. Xie, Qing Zhou, Ying Liu, Samuel Zalipsky, Xiaodong Yang. Systemic Delivery of Therapeutic siRNA: Opportunities & Challenges. Drug Delivery Technology 2009; 9:32-37.
(24) Hu-Lieskovan S, Heidel JD, Bartlett DW, Davis ME, Triche TJ. Sequence-specific knockdown of EWS-FLI1 by targeted, nonviral delivery of small interfering RNA inhibits tumor growth in murine model of metastatic Ewing's sarcoma. Cancer Research 2005; 65:8984-8992.
(25) Landen CN Jr, Chavez-Reyes A, Bucana C, Schmandt R, Deavers MT, Lopez-Berestein G, Sood AK. Therapeutic *EphA2* gene targeting *in vivo* using neutral liposomal small interfering RNA delivery. Cancer Research 2005; 65:6910-6918.
(26) Zimmermann TS, Lee AC, Akinc A, Bramlage B, Bumcrot D, Fedoruk MN, Harborth J, Heyes JA, Jeffs LB, John M, Judge AD, Lam K, McClintock K, Nechev LV, Palmer LR, Racie T, Röhl I, Seiffert S, Shanmugam S, Sood V, Soutschek J, Toudjarska I, Wheat AJ, Yaworski E, Zedalis W, Koteliansky V, Manoharan M, Vornlocher HP, MacLachlan I. RNAi-mediated gene silencing in non-human primates. Nature 2006; 441:111-114.
(27) McCaffrey AP, Meuse L, Pham TT, Conklin DS, Hannon GJ, Kay MA. RNA interference in adult mice. Nature 2002; 418:38-39.
(28) Zou X, Qiao H, Jiang X, Dong X, Jiang H, Sun X. Downregulation of developmentally regulated endothelial cell locus-1 inhibits the growth of colon cancer. J Biomed. Sci. 2008; 16:33.
(29) Moschos SA, Williams AE, Lindsay MA. Cell-penetrating-peptide-mediated siRNA lung delivery. Biochem Soc Trans. 2007; 35:807-810.
(30) Fattal E, Bochot A. Ocular delivery of nucleic acids: antisense oligonucleotides, aptamers and siRNA. Adv. Drug Deliv. Rev. 2006; 58:1203-1223.
(31) Song E, Zhu P, Lee SK, Chowdhury D, Kussman S, Dykxhoorn DM, Feng Y, Palliser D, Weiner DB, Shankar P, Marasco WA, Lieberman J. Antibody mediated in vivo delivery of small interfering RNAs via cell-surface receptors. Nature Biotechnology 2005; 23:709-717.

(32) Urban-Klein B, Werth S, Abuharbeid S, Czubayko F, Aigner A. RNAi mediated gene-targeting through systemic application of polyethylenimine (PEI)-complexed siRNA *in vivo*. Gene Therapy 2005; 12:461-466.
(33) Sørensen DR, Leirdal M, Sioud M. Dag R Sorensen, Marianne Leirdal and Mouldy Sioud. Gene silencing by systemic delivery of synthetic siRNAs in adult mice. J. Mol. Biol. 2003; 327:761-766.
(34) Spagnou S, Miller AD, Keller M. Lipid carriers of siRNA: differences in the formulation, cellular uptake, and delivery with plasmid DNA. Biochemistry 2004; 43:13348-13356.
(35) Morrissey DV, Lockridge JA, Shaw L, Blanchard K, Jensen K, Breen W, Hartsough K, Machemer L, Radka S, Jadhav V, Vaish N, Zinnen S, Vargeese C, Bowman K, Shaffer CS, Jeffs LB, Judge A, MacLachlan I, Polisky B. Potent and persistent in vivo anti-HBV activity of chemically modified siRNAs. Nature Biotechnology 2005; 23:1002-1007.

CHAPTER 2:

NANODISKS SOLUBILIZE THE POLYPHENOL CURCUMIN AND POTENTIATE ITS BIOLOGICAL EFFECTS IN TUMOR CELL LINES

2.1. Abbreviations

AFM = atomic force microscopy
apo = apolipoprotein
DMPC = 1,2-dimyristoyl-*sn*-glycero-3-phosphocholine
DMSO = dimethylsulfoxide
FITC = fluorescein isothiocyanate
MCL = mantle cell lymphoma
NAC = N-acetyl cysteine
ND = nanodisks
PBS = phosphate buffered saline
PI = propidium iodide
ROS = reactive oxygen species

2.2. Abstract

Curcumin is a food additive popular in Southeast Asia. It is a natural polyphenol which possesses diverse pharmacological effects including anti-inflammatory and anti-cancer activities. However, curcumin is water insoluble. Clinical evaluation of this promising compound has been challenging due to its poor bioavailability following oral dosing. Solubilization of curcumin in a suitable delivery vehicle would allow efficient systemic administration of this drug-like compound. Nanodisks (ND) are nanoscale, disk-shaped phospholipid bilayers whose edge is stabilized by apolipoproteins. ND were formulated with curcumin, at a 6:1 phospholipid:curcumin molar ratio. Atomic force microscopy revealed that curcumin-ND are particles with diameters <50 nm and thickness of a phospholipid bilayer. When formulated in ND, curcumin is water-soluble and gives rise to a characteristic absorbance spectrum with a peak centered at 420 nm. Fluorescence spectroscopy of curcumin-ND provided evidence of self-quenching. Incubation of curcumin-ND with empty-ND relieved the self-quenching, indicating re-distribution of curcumin between curcumin loaded- and empty-ND. Curcumin formulated as curcumin-ND caused enhanced growth inhibition in the HepG2 cells. In cell culture models of mantle cell lymphoma (MCL), curcumin-ND were a potent inducer of apoptosis. Flow cytometry analyses revealed production of reactive oxygen species in curcumin-treated MCL cells. Key proteins involved in the apoptotic pathway such as cyclin D1, Akt, phosphorylated IkBα and Bcl2 were down regulated while caspase-9, -3 and PARP cleavage were enhanced in the MCL cells in response to curcumin-ND treatment. In addition, curcumin-ND incubation led to enhanced G_1 cell cycle arrest in two cultured cell models of MCL. The nanoscale size of the complexes, combined with their ability to solubilize curcumin with complete retention of its biological effects, indicate ND may have *in vivo* therapeutic applications.

2.3. Introduction

Curcumin, chemically known as diferuloylmethane, is a hydrophobic polyphenol derived from rhizome of turmeric (*Curcuma longa*), an East Indian plant. Curcumin possesses diverse pharmacologic effects including anti-inflammatory, anti-oxidant and anti-proliferative activities (1-4). Indeed, accumulating experimental evidence indicates curcumin has intrinsic anticancer activity. Furthermore, curcumin is non-toxic, even at relatively high doses (5). Despite this, clinical advancement of this promising molecule has been hindered by poor water solubility, short biological half-life, and low bioavailability following oral administration (6, 7). Attempts to overcome these limitations include synthesis of curcumin analogues (8), the use of adjuvants as well as development of improved delivery platforms such as liposomes and nanoparticles (9-12).

Nanodisks (ND) are nanoscale particles comprised of a disk-shaped lipid bilayer that is stabilized by an apolipoprotein scaffold (13). ND self assemble in solution upon presentation of the scaffold protein to a phospholipid vesicle substrate to which an appropriate hydrophobic bioactive agent has been introduced. The apolipoprotein molecules mediate re-organization of the phospholipid/bioactive agent substrate forming the ternary ND product. The ND structure is stabilized by interaction of the hydrophobic face of amphipathic α-helix segments of the apolipoprotein scaffold with fatty acyl moieties at the edge of the bilayer disk. At the same time, the hydrophilic faces of these helixes are directed towards the aqueous milieu, conferring water solubility to the complex. Previous studies with the polyene antibiotic, amphotericin B (14) and the bioactive isoprenoid, all *trans* retinoic acid (15), showed efficient incorporation into ND, with retention or enhancement of biological activity. Based on the structural properties of curcumin, it was identified as a candidate for formulation into ND. Curcumin-ND were characterized with respect to structural properties and biological activity. Size and morphology of the particles were studied using atomic force microscopy (AFM). Curcumin has been shown to possess anti-proliferative and pro-apoptotic effects towards tumor cells (16-21). Anti-proliferative effect of curcumin-ND was evaluated in HepG2 cells and pro-apoptotic effect was tested on mantle cell lymphoma (MCL) cell lines. Data from these studies establish that ND mediate improved cellular delivery of curcumin which translates into stronger anti-proliferative and apoptotic effects in cultured tumor cells. Mechanistic studies in MCL cells reveal curcumin-ND mediated generation of reactive oxygen species (ROS) induce apoptosis by modulating key proteins involved in the apoptotic pathway. Cyclin D1, Akt, phosphorylated IkBα and Bcl2 were down regulated while caspase-9, -3 and PARP cleavage were enhanced in the MCL cells in response to curcumin-ND treatment. Increased growth arrest at G_1 phase of the cell cycle was also observed.

2.4. Results

Curcumin-ND formulation

Curcumin-ND formulation strategy takes advantage of the unique ability of amphipathic apolipoproteins to transform specific phospholipid vesicle substrates into ND (22). By introducing curcumin into the reaction mix, it was hypothesized that a ternary ND complex, comprised of phospholipid, apolipoprotein and curcumin, would be generated. Ten mg of the phospholipid 1,2-dimyristoyl-*sn*-glycero-3-phosphocholine (DMPC) and 1 mg curcumin (DMPC/ curcumin mole ratio of 5.5:1) were incubated with the apolipoprotein (apo) A-I at 24°C with bath sonication until the sample changed from an opaque, turbid suspension to a clarified solution. After centrifugation, 70% of the original curcumin was recovered in the supernatant fraction (**Table 2-1**). Although phospholipid alone was able to solubilize 60% of the added curcumin, the solution remained turbid. By contrast, only 9% of the original curcumin was recovered in the supernatant when incubated in buffer alone under identical conditions. Overnight dialysis and filtration of the curcumin-ND preparation resulted in negligible loss of curcumin, indicating stable incorporation of this polyphenol into ND. Compositional analysis of the product particles yielded a final DMPC/curcumin mole ratio of 6:1.

Table 2-1. Effects of phospholipid (PL) and ApoA-I on curcumin solubility.

Components*	Solubilization efficiency† (%)
Curcumin + PL + ApoA-I	70
Curcumin + PL	60
Curcumin + Buffer only	9

* The individual components were added to PBS and processed as described in **Methods**. Sample containing curcumin, PL and ApoA-I yielded curcumin-ND.

† Solubilization efficiency (%) = the amount of curcumin in supernatant after centrifugation ÷ curcumin added to the incubation X 100.

Characterization of curcumin-ND by AFM

To examine the shape, morphology and polydispersity of curcumin-ND, AFM experiments were conducted (**Figure 2-1)**. Both empty and curcumin-loaded ND were discoidal in shape. Fully assembled curcumin-ND were uniformly nanoscale in size, with a diameter of 48 +/- 9 nm and thickness of approximately 5.3 +/- 0.8 nm, consistent with the thickness of a single phospholipid bilayer. Control empty ND had a diameter of 49 +/- 15 nm and height of 4.9 +/- 0.7 nm. No particles were found above 60 nm in diameter.

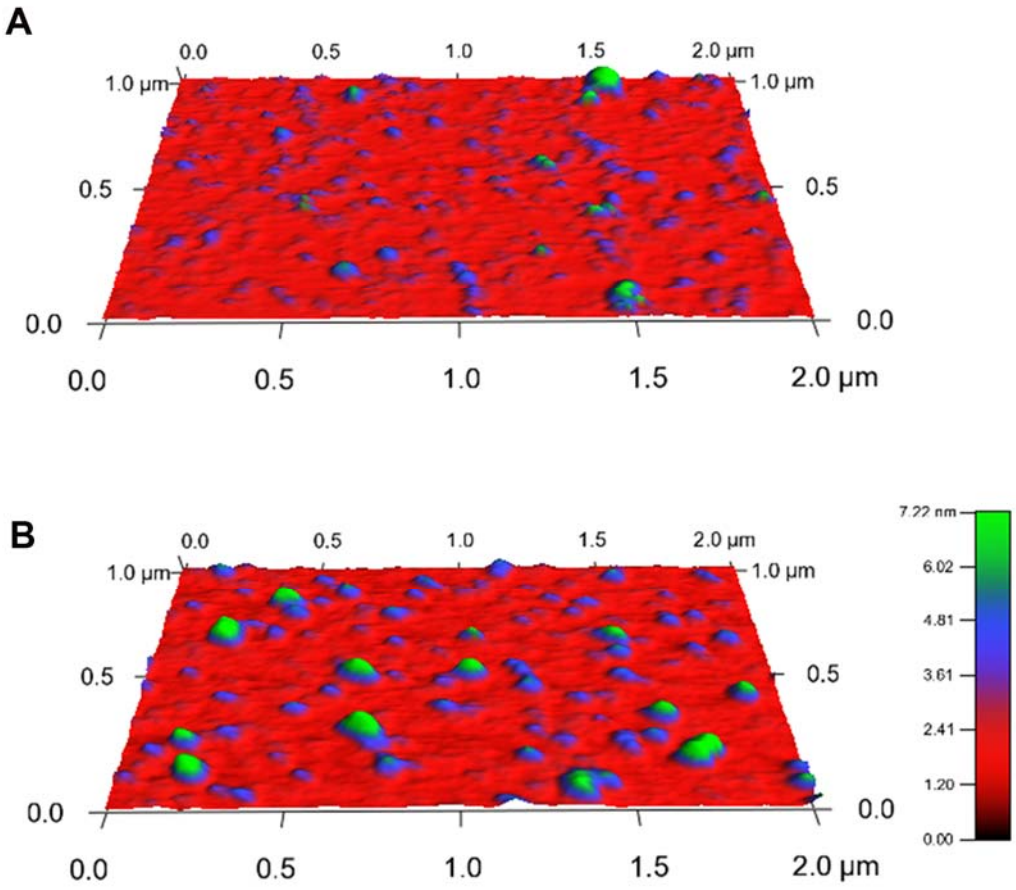

Figure 2-1. AFM of curcumin-ND. Samples were incubated on an atomically flat Muscovite mica surface in imaging buffer (PBS with 10 mM $MgCl_2$) then lightly rinsed. Topographical images were obtained with silicon nitride cantilever probes with a spring constant of 0.05 N/m. (**A**) Empty ND. (**B**) Curcumin-ND. Scale at right represents a color-coded measurement of height (nm).

Spectral properties of curcumin-ND

Curcumin is a yellow colored compound that, upon dissolution in a polar organic solvent (e.g. DMSO) absorbs light in the visible wavelength range. On the contrary, curcumin is insoluble in aqueous media at neutral pH and, as a result, exhibits low absorbance. In agreement with previous studies (23-25), a UV-Vis absorbance spectrum of curcumin in DMSO gave rise to a single major peak centered at 430 nm while the corresponding spectrum of free curcumin in PBS displayed far less absorbance (**Figure 2-2**). In comparison, the spectrum of curcumin-ND in PBS was of similar intensity to that of free curcumin in DMSO, indicating solubilization of curcumin. The spectrum of curcumin-ND also displayed more fine structure, with distinct shoulders on both sides of the absorbance maximum. Furthermore, the absorbance maximum for curcumin-ND was blue shifted to 420 nm indicating curcumin present in ND experiences a relatively non-polar environment.

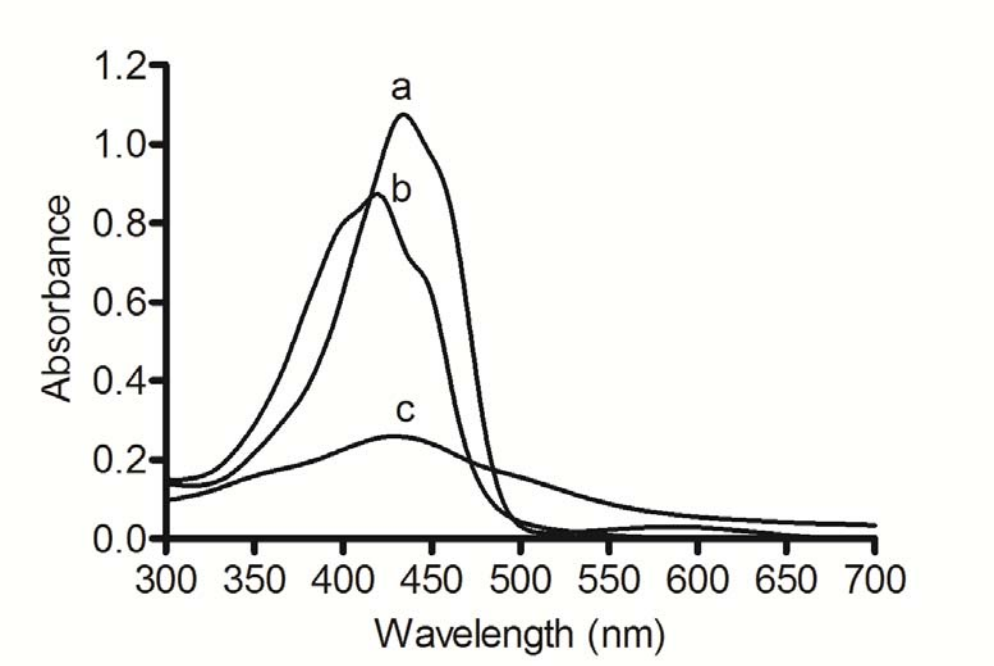

Figure 2-2. UV-Vis Absorbance spectra of curcumin. Twenty μM curcumin as a) free curcumin in DMSO, b) curcumin-ND in PBS and c) free curcumin in PBS were scanned from 300 to 700 nm.

Excitation of free curcumin in DMSO gave rise to an emission peak centered at 520 nm (excitation 420 nm) (**Figure 2-3 A**). Whereas free curcumin in PBS did not fluoresce under these conditions, curcumin-ND in PBS gave rise to an emission spectrum whose intensity was significantly attenuated, compared to curcumin in DMSO. Similar to the absorbance maximum, the fluorescence maximum for curcumin-ND was blue shifted to 500 nm. To examine if the low fluorescence intensity of curcumin-ND was due to self-quenching by curcumin when concentrated in the ND milieu, curcumin-ND were incubated with increasing amounts of empty ND. Consistent with transfer of curcumin from curcumin-ND to the empty ND pool, curcumin fluorescence emission intensity increased as a function of increasing empty ND concentration (**Figure 2-3 B**).

Given the characteristic fluorescence properties of curcumin and its apparent localization in the ND particle milieu, experiments were conducted to assess whether it may affect the intrinsic tryptophan fluorescence properties of the ND scaffold protein, apoA-I. When curcumin-ND were excited at 280 nm and fluorescence emission monitored from 300 - 450 nm, compared to empty ND, apoA-I tryptophan fluorescence was quenched (**Figure 2-3 C**). Control experiments with free curcumin showed no fluorescence upon excitation at 280 nm. This result suggests that when incorporated into ND, curcumin resides in close proximity to the ND scaffold protein, apoA-I.

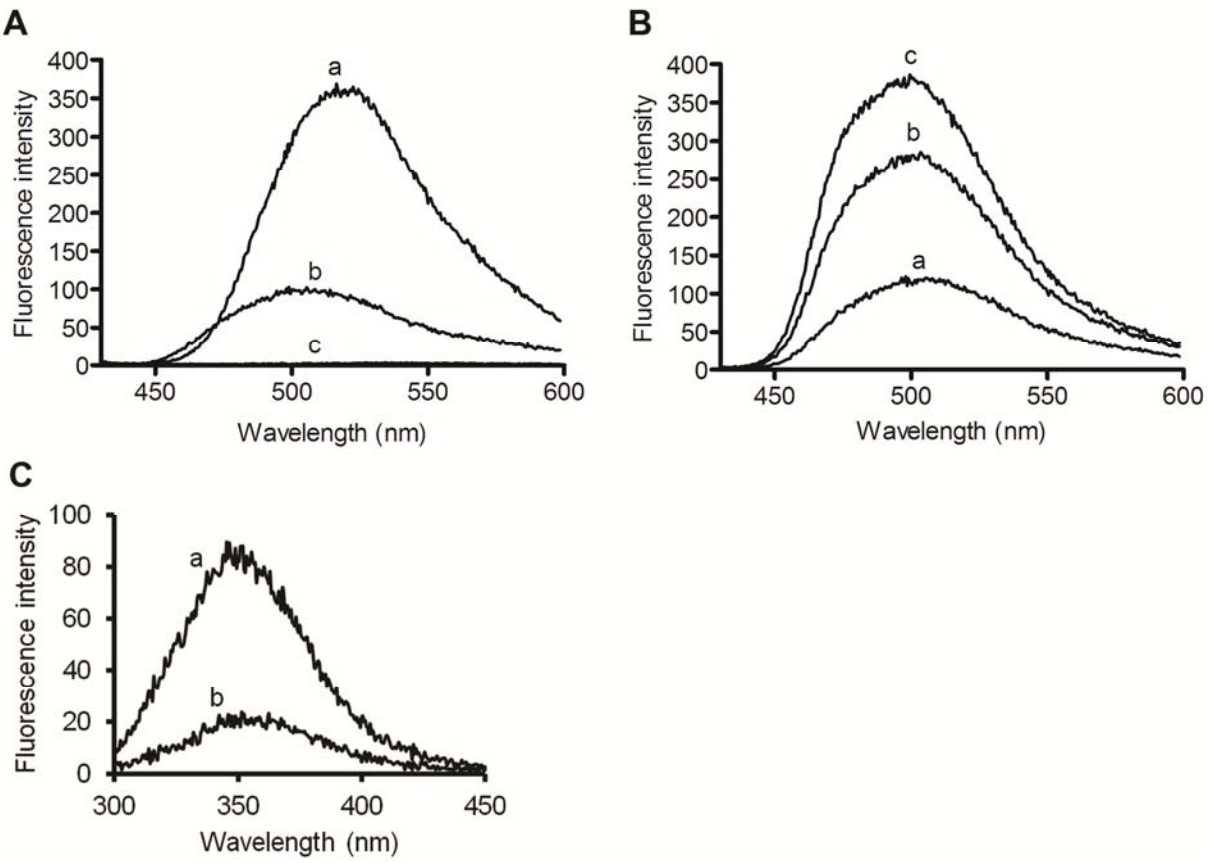

Figure 2-3. Fluorescent properties of curcumin. (**A**) Fluorescence spectroscopy of curcumin. Fifteen μM curcumin as a) free curcumin in DMSO, b) curcumin-ND in PBS and c) free curcumin in PBS were excited at 420 nm and emission scanned from 430 to 600 nm. (**B**) Effect of empty ND on the fluorescence intensity of curcumin-ND. Samples included a) curcumin-ND, b) curcumin-ND plus an equivalent amount of empty ND and c) curcumin-ND plus 2 fold excess empty ND. (**C**) Effect of curcumin on apoA-I tryptophan fluorescence emission intensity. Samples contained equivalent amount of apoA-I (1 μM) and were excited at 280 nm and fluorescence emission monitored from 300 - 450 nm. Samples include a) empty ND, b) curcumin-ND.

Anti-proliferative effect of curcumin on HepG2 cells

To assess the biological activity of curcumin when formulated in ND, hepatoma cells were exposed to culture media supplemented with buffer (control), free curcumin (in DMSO) or curcumin-ND (in PBS) and cell viability determined at 24 and 48 h (**Figure 2-4**). Whereas empty ND had no effect on cell viability, curcumin-ND inhibited hepatoma cell growth more effectively than free curcumin. At both time points and for all three concentrations tested, the difference between curcumin-ND and free curcumin was found to be statistically significant ($P<0.05$).

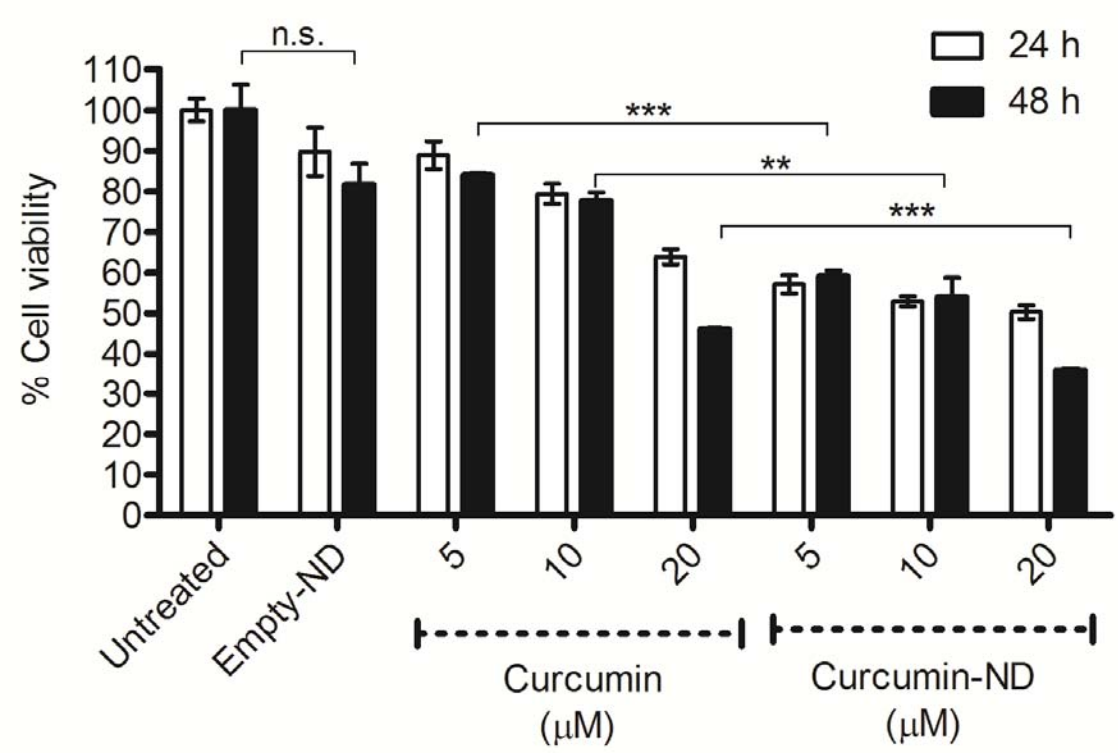

Figure 2-4. Curcumin-ND exhibit potent anti-proliferative effect on HepG2 cells. Cells were incubated with specified concentrations of free curcumin (in DMSO) or curcumin-ND for 24 and 48 h. Percent cell viability, relative to untreated cells, was measured by MTT assay. Values are reported as mean ± S.D. (n=4). At both time-points, for all three concentrations tested, the difference between curcumin-ND and free curcumin was statistically significant. Differences between groups for the 48 h time point are shown in the figure. ** $P<0.01$; *** $P<0.001$; n.s. not significant.

Mechanism for curcumin's pro-apoptotic effect on MCL cells

[Data was collected in the laboratory of Dr. Leo I. Gordon of Northwestern University]

Two different MCL cell lines, Jeko and Granta, were used to compare pro-apoptotic effect of curcumin-ND versus free curcumin. Jeko and Granta cells were incubated with medium alone (control), free curcumin, empty ND and curcumin-ND followed by measurement of apoptosis by FACS (**Figure 2-5**). Compared to medium alone, empty ND had no effect on the number of apoptotic cells. By contrast, curcumin-ND produced a concentration-dependent increase in apoptosis. Indeed, at 20 μM, curcumin-ND induced a much greater apoptotic response than free curcumin for both MCL cell lines.

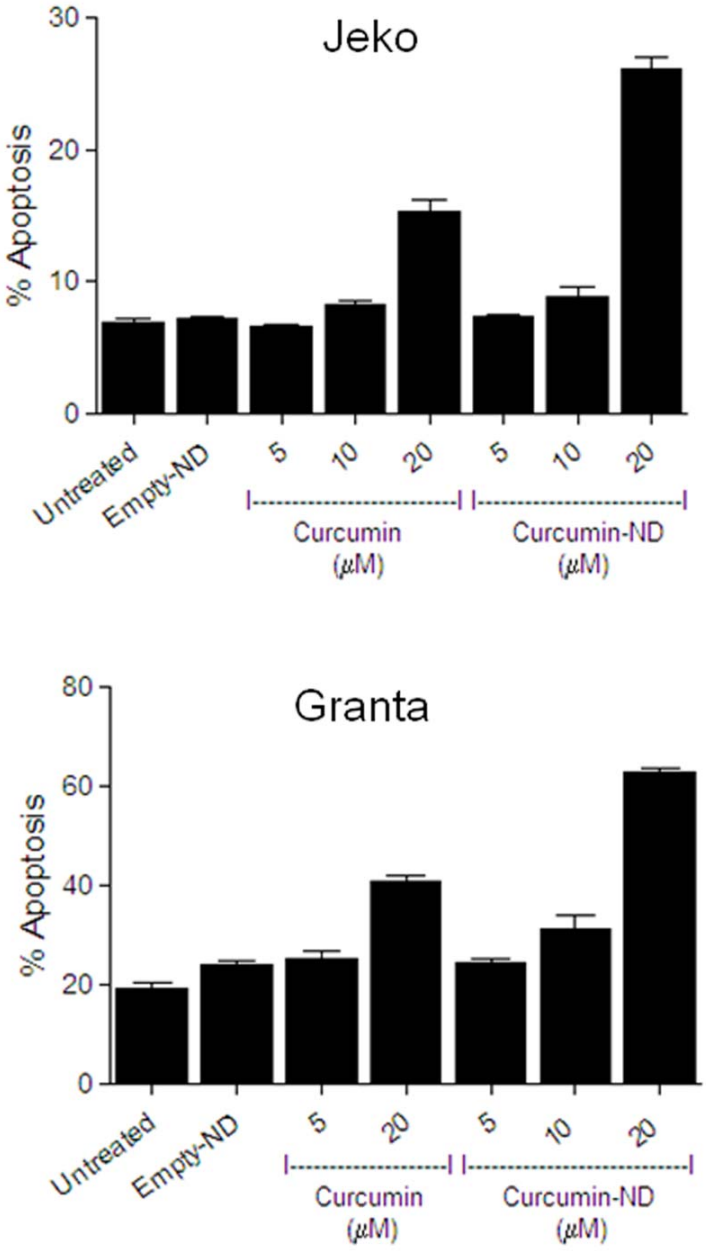

Figure 2-5. Curcumin-ND is a more potent inducer of apoptosis in MCL cells. Cells were incubated for 24 h with different concentrations of free curcumin (in DMSO) or curcumin-ND. Apoptosis was measured by flow cytometry**.** Early and late apoptotic percentages (AnnexinV/PI positive) from dot plots were combined to estimate total apoptosis. Values shown are the mean ± SD (n = 3). For both cell lines, $P<0.001$ for curcumin-ND versus free curcumin at 20 μM curcumin concentration.

Several drugs used in chemotherapy induce cell death via ROS generation (26). To examine if curcumin-ND induce ROS generation in cultured MCL cells, Granta and NCEB cells were treated with curcumin-ND and intracellular ROS measured as a function of time. In Granta, ROS levels increased as early as 1 h, and declined after 3 h following incubation with curcumin-ND (**Figure 2-6 A**). In NCEB cells, however, ROS increased at 1 h and was sustained over a 6 h period. When Granta cells were co-incubated with the antioxidant and ROS scavenger, N-acetylcysteine (NAC), curcumin-ND induced apoptosis was prevented (**Figure 2-6 B**).

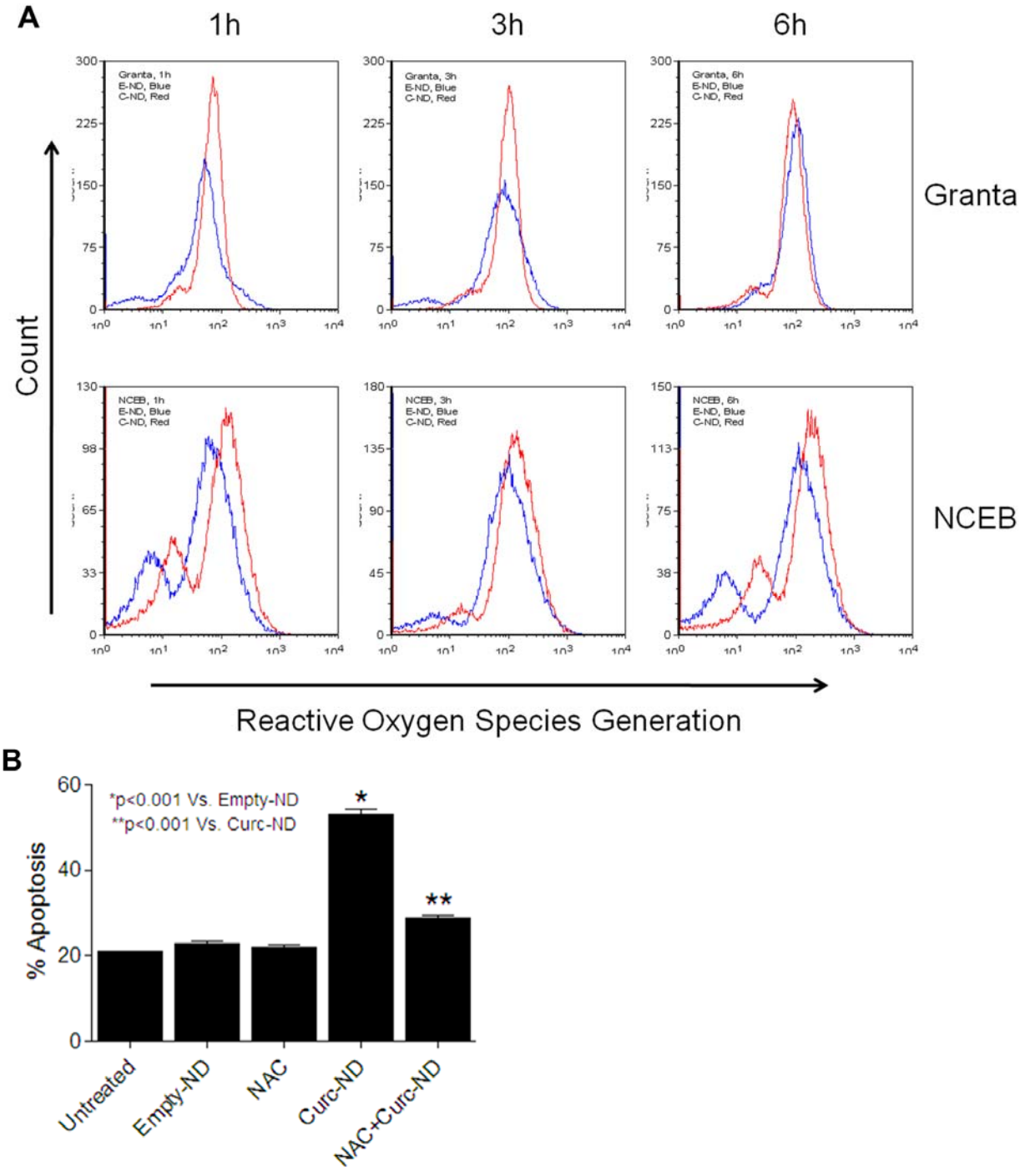

Figure 2-6. Effect of curcumin-ND on ROS generation in MCL cells. (**A**) Granta and NCEB cells were treated with 20 μM curcumin-ND and empty-ND for 1, 3, and 6 h at 37 °C. ROS production in live cells was measured by flow cytometry as described in 'Methods'. In the two cell lines, there is an increase in ROS after curcumin-ND treatment (red trace on the graph) compared with empty-ND (blue trace). (**B**) Granta cells were incubated with medium alone (untreated), empty-ND, NAC (10 mM), Curcumin-ND (20

μM), and combination of curcumin-ND and NAC. Cells were pretreated with NAC for 4 h before adding curcumin-ND. After 48 h, cells were analyzed for apoptosis by Flow Cytometry as described in Methods. Early and late apoptotic percentages (AnnexinV/PI positive) from each dot plot were combined to represent total apoptosis (summarized in the bar graph; n = 3).

To investigate the mechanism underlying curcumin-ND induced apoptosis, its effects on apoptosis-related proteins were studied. Following exposure to curcumin-ND, there was a time-dependent decrease in caspase-9 levels (**Figure 2-7 A**). Furthermore, 16 h after exposure to curcumin-ND caspase-3 was undetectable. Loss of this band implies its activation, which was confirmed by PARP cleavage, wherein a decrease in the 116 kD band was accompanied by an increase in its 85 kD cleavage product. Curcumin-ND induced sustained PARP cleavage, even at 16 h of incubation**,** suggesting continuous release of curcumin from the ND delivery vehicle. Constitutive activation of NF-κB has been reported in a variety of cancers including lymphoid malignancies (18, 27). In cultured Granta cells within 2 h after exposure to curcumin-ND IkBα phosphorylation was decreased while IkBα protein levels were unchanged (**Figure 2-7 B)**. Bcl2 is an anti-apoptotic protein that is overexpressed in MCL cells (28, 29). Consistent with its effects on apoptosis, curcumin-ND suppressed Bcl2 expression in Granta cells at 2 h (**Figure 2-7 C**). Whereas constitutive phosphorylation of Akt is implicated in survival and pathogenesis of MCL (30), the effect of curcumin-ND on pAkt levels is unknown and hence, was examined. As shown in **Figure 2-7 C**, between 2 and 8 h following treatment curcumin-ND induced a decrease in pAkt levels. Since cyclin D1 is also overexpressed in MCL cells, the levels of this protein were investigated as a function of time following exposure to curcumin-ND. Curcumin-ND induced a decrease in cyclin D1 expression (**Figure 2-7 D**).

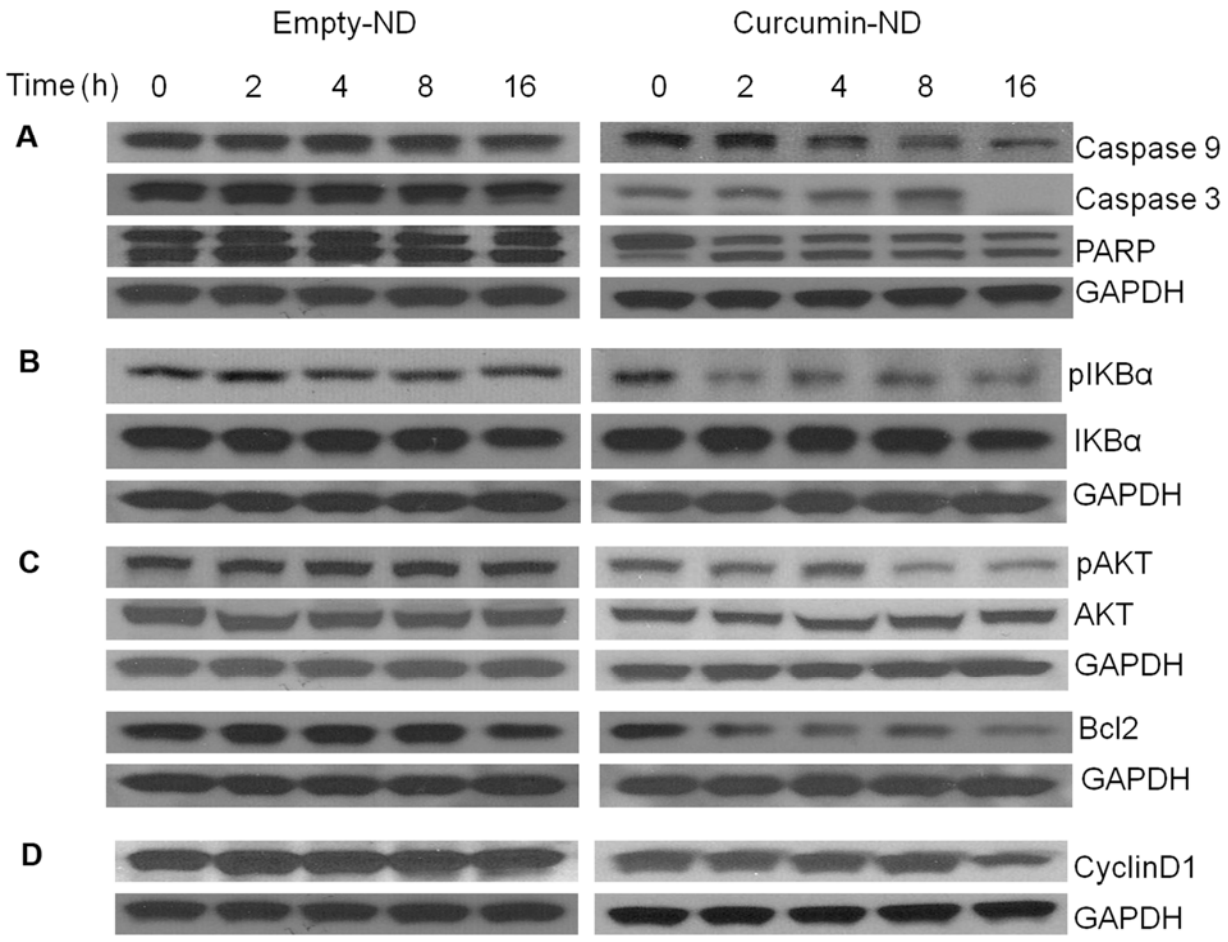

Figure 2-7. Effect of curcumin-ND on apoptosis marker proteins. Granta cells were incubated with empty-ND or 20 μM curcumin-ND for specified times. Following incubation, cell homogenates were separated by SDS-PAGE, transferred to nitrocellulose and probed with antibodies directed against caspase-9, caspase-3, PARP and GAPDH (**A**), pIKBα, IKBα, GAPDH (**B**), pAkt, Akt, Bcl2, GAPDH (**C**), and Cyclin D1 and GAPDH (**D**).

Since curcumin-ND incubation led to a decrease in cyclin D1 levels, its effects on cell cycle progression in Granta and Jeko cells were examined. As seen in **Figure 2-8**, in both cell lines, curcumin-ND induced G_1 cell cycle arrest.

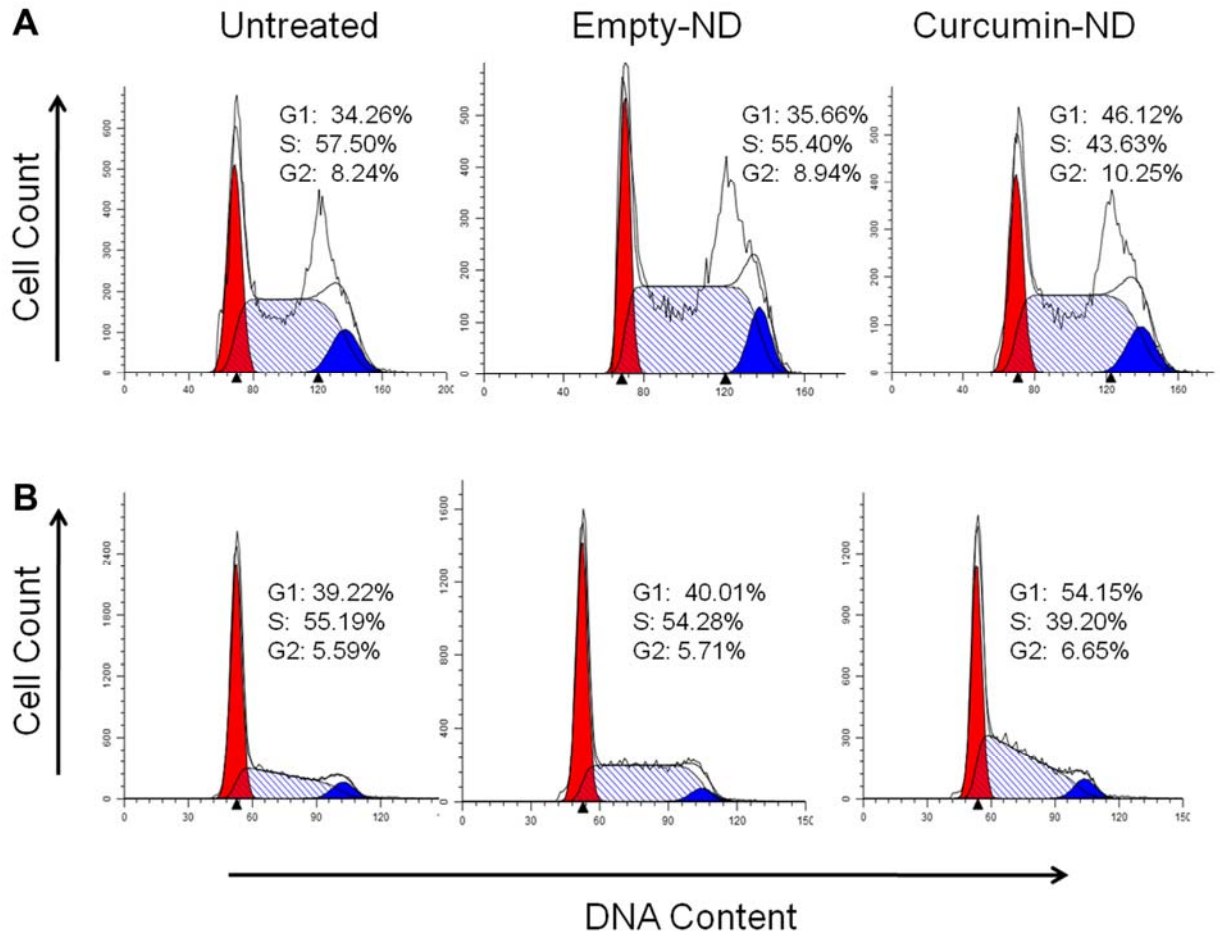

Figure 2-8. Effect of curcumin on MCL cell cycle progression. Granta (**A**) and Jeko (**B**) cells were incubated for 24 h with medium alone (untreated), empty-ND, or curcumin-ND (20 μM). Following incubation, cells were analyzed for DNA content as described in Methods. The percentage of cells in G_1, S, and G_2 were evaluated using ModFit LT for Win32 software (Verity Software House, Topsham, ME). G_1 (red), G_2 (blue), and S (hatched).

2.5. Discussion

Incorporation of curcumin into ND overcomes the poor water solubility of this bioactive molecule. The particles generated are nanoscale, disk-shaped complexes of curcumin, DMPC and apoA-I. Application of ND as a drug delivery vehicle has been explored in our laboratory with other water-insoluble bioactive compounds. For example, incorporation of the polyene antibiotic, amphotericin B, into ND generates similar sized particles that show efficacy in mice infected with the pathogenic fungus, *Candida albicans* (14) as well as the protozoal parasite, *Leishmania major* (31). Likewise, ND formulated with the lipophilic retinoid, all *trans* retinoic acid, induce apoptosis in cell models of Mantle cell lymphoma (32). When considered in the light of the present data, it may be concluded that ND provide a broad platform for hydrophobic bioactive agent delivery.

When taken orally, poor absorption / bioavailability severely limits the clinical utility of curcumin (33). The data presented herein show that curcumin can be solubilized by stable integration into ND. The observation that curcumin-ND not only retains, but potentiates, the biological activity of curcumin in hepatoma cells and lymphoma cells, indicates that curcumin itself has not been altered during formulation or as a result of its association with ND. In fact, data shows that curcumin-ND are more potent in killing HepG2 cells compared to free curcumin. Curcumin, formulated as curcumin-ND was also found to be a more potent inducer of apoptosis in cultured MCL cells. Curcumin-ND incubation with cultured MCL cells induced ROS generation. Given that the antioxidant, N-acetylcysteine, inhibits curcumin-ND induced effects on apoptosis, it may be concluded that ROS generation in response to curcumin is involved in the cell death pathway. Furthermore, the observed effects of curcumin in general are consistent with results reported for SP-53 cells (18), osteosarcoma (34) and lymphoma cells (35). Apoptosis, cell cycle and immune responses are regulated in large part by NF-κB. Constitutive activation of NF-κB has been reported in a variety of cancers, including lymphoid malignancies (18, 27). In unstimulated cells, NFκB is sequestered in the cytoplasm as an inactive heterotrimer consisting of p50, p65, and IκBα subunits. Upon activation, IκBα becomes phosphorylated, ubiquitinylated and, ultimately, degraded (36). Upon activation, NFκB translocates to the nucleus where it serves to activate target genes regulated by κB sites. In Granta cells, we examined the effect of curcumin-ND on the phosphorylation status of IκBα and found that, within 2 h after exposure to curcumin-ND, IκBα phosphorylation was inhibited. This result is consistent with a previous study of the effects of curcumin on IκBα phosphorylation in cultured MCL cells (18). Importantly, however, when presented to the cells as curcumin-ND, the onset of inhibition was earlier and the down-regulation was sustained. In a similar manner, compared to free curcumin (18), curcumin-ND led to an earlier onset of suppression of Bcl2 expression in Granta cells. Consistent with a classical apoptotic response, curcumin-ND also induced down-regulation of cyclin D1, decreased phosphorylation of Akt, enhanced cleavage of caspases-9 and -3, and PARP. Furthermore, curcumin-ND induced G_1 cell cycle arrest in two cultured cell models of MCL.

Taken together, the data indicate that formulation of curcumin into ND enhances and prolongs its biological effects. ND represent a potentially novel means for effective delivery of curcumin to specific tissues or cell types. The possibility of targeting ND by engineering its apolipoprotein scaffold makes it a versatile delivery platform (37). Given the water solubility of this formulation, it is amenable to intravenous infusion, thereby bypassing the poor bioavailability of oral curcumin. In light of the results obtained, further investigation of the in vivo efficacy of curcumin-ND, in isolation or as a combination therapy, is warranted.

2.6. Methods

Materials

Curcumin was obtained from Cayman Chemical (Ann Arbor, MI) and used without further purification. Dimyristoylphosphatidylcholine (DMPC) was obtained from Avanti Polar Lipids Inc (Alabaster, AL). The ND scaffold protein, recombinant apolipoprotein (apo) A-I, was expressed in E. coli and isolated as described previously (22). CellTiter 96 Non-Radioactive Cell Proliferation (MTT) Assay kit was obtained from Promega (Madison, WI). FITC-annexin-V Apoptosis kit was obtained from Invitrogen (Carlsbad, CA). 2',7'-dichlorodihydrofluorescein diacetate (H2DCFDA) was purchased from Molecular Probes, Inc. (Carlsbad, CA) and propidium iodide (PI) was from Biosource (Camarillo, CA). The following antibodies were used: PARP, caspases 9 and 3, pIκBα, IκBα, BCl2, Akt, pAkt (Cell Signaling), cyclin D1 (Santa Cruz), and GAPDH (Chemicon).

Cell culture

HepG2 cells were obtained from American Type Culture Collection. HepG2 cells were cultured in minimal essential medium supplemented with 0.1 mM non-essential amino acids, 1 mM sodium pyruvate, and 10% fetal bovine serum at 37°C in a humidified atmosphere of 5% CO_2 and 95% air. MCL cells (Jeko, Granta and NCEB) were cultured in RPMI-1640 containing 10% fetal bovine serum, 1% sodium pyruvate and in the presence of penicillin, streptomycin, and glutamine at 37°C in a humidified atmosphere of 5% CO_2 and 95% air.

Curcumin-ND preparation

Ten mg DMPC was dissolved in chloroform / methanol (3:1 v/v) and dried under a stream of N_2 gas, forming a thin film on the vessel wall. Residual organic solvent was removed under vacuum. The prepared lipids were then dispersed in 1.2 ml phosphate buffered saline (PBS; 20 mM sodium phosphate, 150 mM sodium chloride, pH 7.0) and 1.0 mg curcumin (from a stock solution in dimethylsulfoxide; DMSO) was added. Following this, 4 mg apoA-I (6.5 - 7 mg/ml in PBS) was added and the solution (2.0 ml final volume) subjected to bath sonication under a N_2 atmosphere, with the sample temperature maintained between 22°C and 25°C. After sonication the turbid mixture became clear, indicating apolipoprotein/phospholipid complexes (e.g. ND) had formed. For solubilization efficiency calculations, the curcumin-ND preparation was centrifuged at 14,000 rpm for 10 minutes to pellet unincorporated curcumin, followed by determination of curcumin content in the supernatant. The preparation was further dialyzed (MWCO 6 - 8 kDa) against PBS for 16 h to remove DMSO, followed by 0.22 μm filter sterilization to remove particles larger than 220 nm. The phospholipid and curcumin content of the preparation was determined to calculate the final

DMPC/curcumin mole ratio. Empty ND were prepared as described above except that curcumin was omitted.

Quantitation of curcumin

A 4 mg/ml stock solution of curcumin was prepared in DMSO. A standard curve, generated by serial dilution of the stock solution in a 96-well microplate format, was used to determine curcumin concentrations in unknown samples following transfer of an aliquot to DMSO. Sample absorbance was measured at 430 nm on SpectraMax 340 plate reader (Molecular Devices, CA).

Analytical procedures

Protein concentrations were determined by the bicinchoninic acid assay (Pierce Chemical Co.) with bovine serum albumin as standard. DMPC was quantified by enzyme based colorimetric Phospholipids C assay (Wako Chemicals USA).

AFM

AFM was used to determine size and morphology of curcumin loaded- and empty- ND. Two µL of solution containing ND (10 ng/mL) was incubated for two minutes on atomically flat Muscovite mica surface in imaging buffer (phosphate buffered saline plus 10 mM $MgCl_2$), then lightly rinsed. Topographical images were obtained with silicon nitride cantilever probes (MSCT, Veeco, Santa Barbara, CA) with a spring constant of 0.05 N/m. Images were taken in alternate contact mode in liquid, with amplitudes below 20 nm and an amplitude set point at 50% tapping amplitude. Scan rates were below 1.0 Hz. Height and amplitude of images were recorded. Diameters of particles in images were determined by full width half maximum analysis of contiguous particles in the slow scan direction, using IgorPro Wavemetrics software routines. Experiments were carried out at 22 +/- 1°C.

UV/Vis absorbance spectroscopy

Absorbance spectroscopy was performed on a Perkin-Elmer Lambda 20 spectrophotometer. Samples were scanned from 300 - 700 nm.

Fluorescence spectroscopy

Fluorescence spectra were obtained on a Perkin-Elmer LS 50B luminescence spectrometer. Curcumin samples were excited at 420 nm and emission was monitored from 430 - 600 nm (2.5 nm slit width). Tryptophan residues in the ND scaffold protein

(apoA-I) were excited at 280 nm and emission monitored from 300 - 450 nm (2.5 nm slit width).

Cell proliferation assay

HepG2 cells were plated in 96 well culture plates at 3000 cells per well and allowed to attach overnight. After 24 h, the medium was replaced with fresh medium supplemented with specified concentrations of free curcumin (in DMSO), curcumin-ND or empty ND. Twenty four and 48 h after treatment, cell proliferation assays were performed as described by the manufacturer. Briefly, cells were incubated with MTT (3-[4,5-dimethylthiazol-2-yl]-2,5-diphenyltetrazolium bromide) for 2 h at 37°C. MTT is reduced to the water insoluble, colored product, formazan, by metabolically active cells. Formazan is dissolved in solubilization buffer provided by the manufacturer and absorbance read at 570 nm. Values expressed are the mean ± S.D. (n = 4) percent cell viability relative to untreated cells.

Apoptosis measurement

Cellular apoptosis was measured by flow cytometry (32, 39)**.** In brief, cells were incubated with free curcumin, curcumin-ND or empty ND for 24 h, washed with ice cold PBS and re-suspended in binding buffer containing 2.5 µl FITC-annexin V and 5.0 µl propidium iodide for 15 minutes at 37°C in a CO_2 incubator. Subsequently, flow cytometry measurements were obtained on a Beckman Coulter EPICS XL-MCL Cytometer. All experiments were performed in triplicate.

Cell Cycle Progression Assay

Cells were incubated with curcumin-ND or empty-ND or medium alone (untreated) for 24 h (32). Cells were fixed in 70% ethanol, washed, resuspended in 0.5 mL DNA extraction buffer (0.2 M Na_2HPO_4 in 0.1 M citric acid, pH 7.8) and centrifuged. The pellet was resuspended in 1 mL PBS containing PI (50 µg/mL) and ribonuclease A (200 µg/mL) and incubated at 37°C for 20 minutes in the dark. The percentage of cells in G_1, S, and G_2 was evaluated using ModFit LT for Win32 software (Verity Software House, Topsham, ME).

Reactive Oxygen Species

ROS production was measured by flow cytometry (32). Granta and NCEB cells were seeded at a density of 0.5 x 10^6 cells/well in 24 well plates and treated with curcumin-ND (20 µM) or empty-ND for 1, 3, and 6 h. Cells were then stained with 5 µM H_2DCFDA and 2 µg PI per well and incubated for 30 minutes at 37 °C in a humidified CO_2 incubator. Cells were washed with PBS and ROS were measured by flow

cytometry with a Beckman Coulter EPICS XL-MCL Cytometer. In some studies cells were treated with the ROS scavenger, NAC. All experiments were performed in triplicate.

Western Blotting

Fifty µg protein was subjected to SDS-PAGE, transferred to a nitrocellulose membrane and probed with specified antibodies. Immune complexes were visualized by enhanced chemiluminescence.

Statistics

Data from cell proliferation and apoptosis assays were expressed as percent viable cells (viability after treatment with either free curcumin or curcumin-ND over viability after treatment with media only) and percent apoptotic cells (annexin V positive and PI positive over total cells) respectively. Data from ROS measurements in live cells were analyzed and expressed as mean fluorescence. For cell proliferation assay, differences between groups were analyzed by the unpaired Student's *t*-test using Prism 5 software (Graphpad software, La Jolla, CA). $P<0.05$ was considered as significant ($^{*}P<0.05$; $^{**}P<0.01$; $^{***}P<0.001$). For apoptosis and ROS measurements, statistical analysis was performed by one-way ANOVA and Newman-Keuls multiple comparison test (GraphPad Software, Inc., San Diego, CA).

2.7. References

(1) Jurenka JS. Anti-inflammatory properties of curcumin, a major constituent of Curcuma longa: a review of preclinical and clinical research. Alternative Medicine Review 2009; 14:141-153.
(2) Epstein J, Sanderson IR, Macdonald TT. X. Curcumin as a therapeutic agent: the evidence from in vitro, animal and human studies. Br J Nutr 1994; 26:1-13.
(3) Kunnumakkara AB, Anand P, Aggarwal BB. Curcumin inhibits proliferation, invasion, angiogenesis and metastasis of different cancers through interaction with multiple cell signaling proteins. Cancer Letters 2008; 269:199-225.
(4) Hatcher H, Planalp R, Cho J, Torti FM, Torti SV. Curcumin: from ancient medicine to current clinical trials. Cell Mol Life Sci 2008; 65:1631-1652.
(5) Strimpakos AS, Sharma RA. Curcumin: preventive and therapeutic properties in laboratory studies and clinical trials. Antioxidants and Redox Signaling 2008; 10:511-545.
(6) Anand P, Kunnumakkara AB, Newman RA, Aggarwal BB. Bioavailability of curcumin: problems and promises. Molecular pharmaceutics 2007; 4:807-818.
(7) Bisht, S, Maitra A. Systemic delivery of curcumin: 21st century solutions for an ancient conundrum. Curr Drug Discov Technol 2009; 6:192-199.
(8) Agrawal DN, Mishra PK. Curcumin and its analogues: potential anticancer agents. Medicinal Research Reviews 2010; 30:818-860.
(9) Bisht S, Feldmann G, Soni S, Ravi R, Karikar C, Maitra A, Maitra A. Polymeric nanoparticle-encapsulated curcumin ("nanocurcumin"): a novel strategy for human cancer therapy. Journal of Nanobiotechnology 2007; 5:3.
(10) Marczylo TH, Verschoyle RD, Cooke DN, Morazzoni P, Steward WP, Gescher AJ. Comparison of systemic availability of curcumin with that of curcumin formulated with phosphatidylcholine. Cancer Chemother Pharmacol 2007; 60:171-177.
(11) Narayanan NK, Nargi D, Randolph C, Narayanan BA. Liposome encapsulation of curcumin and resveratrol in combination reduces prostate cancer incidence in PTEN knockout mice. Int J Cancer 2009; 125:1-8.
(12) Thangapazham RL, Puri A, Tele S, Blumenthal R, Maheshwari RK. Evaluation of a nanotechnology based carrier for delivery of curcumin in prostate cancer cells. Int J Oncol 2008; 32:1119-1123.
(13) Ryan RO. Nanodisks: hydrophobic drug delivery vehicle. Expert Opin Drug Deliv 2008; 5:343-351.
(14) Oda MN, Hargreaves PL, Beckstead JA, Redmond KA, van Antwerpen R, Ryan RO. Reconstituted high-density lipoprotein enriched with the polyene antibiotic, amphotericin B. J Lipid Res 2006; 47:260-267.
(15) Redmond KA, Nguyen TS, Ryan RO. All-trans retinoic acid nanodisks. Int J Pharm 2007; 339:246-250.
(16) Choudhuri T, Pal S, Das T, Sa G. Curcumin selectively induces apoptosis in deregulated cyclin D1-expressed cells at G2 phase of cell cycle in a p53-dependent manner. J Biol Chem. 2005; 280:20059-20068.
(17) Darvesh AS, Aggarwal BB, Bishayee A. Curcumin and liver cancer: a review. Curr Pharm Biotechnol. 2012; 13:218-228.

(18) Shishodia S, Amin HM, Lai R, Aggarwal BB. Curcumin (diferuloylmethane) inhibits constitutive NF-kappaB activation, induces G1/S arrest, suppresses proliferation, and induces apoptosis in mantle cell lymphoma. Biochem Pharmacol. 2005; 70:700-713.
(19) Hussain AR, Ahmed M, Al-Jomah NA, Khan AS, Manogaran P, Sultana M, Abubaker J, Platanias LC, Al-Kuraya KS, Uddin S. Curcumin suppresses constitutive activation of nuclear factor-KB and requires functional Bax to induce apoptosis in Burkitt's lymphoma cell lines. Mol Cancer Ther. 2008; 7:3318-3329.
(20) Tan TW, Tsai HR, Lu HF, Lin HL, Tsou MF, Lin YT, Tsai HY, Chen YF, Chung JG. Curcumin-induced cell cycle arrest and apoptosis in human acute promyelocytic leukemia HL-60 cells via MMP changes and caspase-3 activation. Anticancer Res. 2006; 26:4361-4371.
(21) Bharti AC, Donato N, Singh S, Aggarwal BB. Curcumin (diferuloylmethane) down-regulates the constitutive activation of nuclear factor-kappa B and IkappaBalpha kinase in human multiple myeloma cells, leading to suppression of proliferation and induction of apoptosis. Blood. 2003; 101:1053-1062.
(22) Ryan RO, Forte TM, Oda MN. Optimized bacterial expression of human apolipoprotein A-I. Protein Expr Purif 2003; 27:98-103.
(23) Chignell CF, Bilski P, Reszka KJ, Motten AG, Sik RH, Dahl TA. Spectral and photochemical properties of curcumin. Photochemistry and Photobiology 1994; 59:295-302.
(24) Khopde SM, Priyadarsini I, Palit DK, Mukherjee T. Effect of solvent on the excited-state photophysical properties of curcumin. Photochemistry and Photobiology 2000; 72:625-631.
(25) Jasim F, Ali F. Measurement of some spectrophotometric parameters of curcumin in 12 polar and nonpolar organic solvents. Microchemical Journal 1989; 39:156-159.
(26) Fruehauf JP, Meyskens FL, Jr. Reactive oxygen species: a breath of life or death? Clin Cancer Res 2007; 13:789-794.
(27) Kim SW, Oleksyn DW, Rossi RM, et al. Protein kinase C-associated kinase is required for NF-nB signaling and survival in diffuse large B-cell lymphoma cells. Blood 2008; 111:1644-1653.
(28) Rummel MJ, de Vos S, Hoelzer D, et al. Altered apoptosis pathways in mantle cell lymphoma. Leuk Lymphoma 2004; 45:49-54
(29) Agarwal B, Naresh KN. Bcl-2 family of proteins in indolent B-cell non-Hodgkin's lymphoma: study of 116 cases. Am J Hematol. 2002; 70:278-282.
(30) Rudelius M, Pittaluga S, Nishizuka S, Pham TH, Fend F, Jaffe ES, Quintanilla-Martinez L, Raffeld M. Constitutive activation of Akt contributes to the pathogenesis and survival of mantle cell lymphoma. Blood. 2006; 108:1668-1676.
(31) Nelson KG, Bishop JV, Ryan RO, Titus R. Nanodisk-associated amphotericin B clears Leishmania major cutaneous infection in susceptible BALB/c mice. Antimicrob Agents Chemother 2006; 50:1238-1244.
(32) Singh ATK, Evens AM, Anderson RJ, Beckstead JA, Sankar N, Bhalla S, Yang S, Forte TM, Ryan RO, Gordon LI. All trans retinoic acid nanodisks enhance retinoic acid receptor-mediated apoptosis and cell cycle arrest in mantle cell lymphoma. Brit J Haemotol 2010; 150:158-169.

(33) Dhillon N, Aggrawal BB, Newman RA, Wolff RA, Kunnumakkara AB, Abbruzzese JL, et al. Phase II trial of curcumin in patients with advanced pancreatic cancer. Clin Cancer Res 2008; 14:4491-4499.
(34) Lee DS, Lee MK, Kim JH. Curcumin induces cell cycle arrest and apoptosis in human osteosarcoma (HOS) cells. Anticancer Res. 2009; 29:5039-5044.
(35) Uddin S, Hussain AR, Manogaran PS, Al-Hussein K, Platanias LC, Gutierrez MI, Bhatia KG. Curcumin suppresses growth and induces apoptosis in primary effusion lymphoma. Oncogene. 2005; 24:7022-7030.
(36) Chen ZJ, Parent L, Maniatis T. Site-specific phosphorylation of InBa by a novel ubiquitination-dependent protein kinase activity. Cell 1996; 84:853-862.
(37) Iovannisci DM, Beckstead JA, Ryan RO. Targeting nanodisks via a single chain variable antibody -apolipoprotein chimera. Biochem Biophys Res Commun 2009; 379:466-469.
(38) Singh ATK, Evens AM, Prachand SN, Gordon LI. Motexafin Gadolinium enhances p53-Mdm2 interactions, reducing p53 and downstream targets in lymphoma cell lines. Anticancer Research 2010; 30:1131-1136.

CHAPTER 3:

APOLIPOPROTEIN E MEDIATED ENHANCED CURCUMIN DELIVERY TO GLIOMA CELLS: EVIDENCE FOR TARGETED DELIVERY WITH NANODISKS

3.1. Abbreviations

apo = apolipoprotein
DMPC = 1,2-dimyristoyl-*sn*-glycero-3-phosphocholine
DMSO = dimethylsulfoxide
FACS = fluorescence activated cell sorting
FITC = fluorescein isothiocyanate
MCL = mantle cell lymphoma
ND = nanodisks
PBS = phosphate buffered saline
PI = propidium iodide

3.2. Abstract

Curcumin, the naturally occurring polyphenol, possesses potent anti-proliferative and anti-oxidant properties. However, therapeutic application of this promising molecule has been challenging due to its water insolubility and poor oral bioavailability. Incorporation of curcumin into nanodisks (ND) overcomes these impediments. In the present study we sought to evaluate ND's ability to interact specifically with cell surface receptors via its scaffold protein and the subsequent effects on curcumin delivery to cells. To address this, curcumin-ND were assembled with apolipoprotein (apo) A-I or E as the scaffold protein and presented to cultured glioblastoma multiforme (GBM) cells. GBM cells express increased amounts of heparan sulfate proteoglycans and receptors of the low-density lipoprotein receptor (LDLR) family for which apoE is a known ligand. Compared to free curcumin, greater cell uptake occurred when curcumin was packaged into ND. Furthermore, an enhancement in curcumin uptake was observed for the apoE curcumin-ND compared to apoA-I curcumin-ND formulation. To determine if increased curcumin uptake by these cells translates into enhanced biological activity, the effect of curcumin on GBM cell viability was examined. At 5 and 10 μM curcumin, apoE curcumin-ND induced greater cell death than either apoA-I curcumin-ND or free curcumin. Furthermore, compared to apoA-I curcumin-ND or free curcumin, apoE curcumin-ND was a more potent inducer of apoptosis in cultured GBM cells. Confocal fluorescence microscopy was used to investigate curcumin's itinerary in GBM cells. One h after exposure of GBM cells to apoE curcumin-ND, significant curcumin uptake was detected while apoE was localized at the cell surface. After 2 h, a portion of the curcumin had migrated to the nucleus, giving rise to enhanced fluorescence intensity in discrete intra-nuclear sites. Z-stack confocal images acquired after 24 h showed that the intra-nuclear sites of curcumin fluorescence remained but did not co-localize with propidium iodide fluorescence. The results suggest an apoE-dependent interaction of ND with GBM cells facilitates curcumin off-loading and cell uptake, resulting in enhanced biological activity.

3.3. Introduction

Interest in curcumin has grown in recent years based on putative pharmacological effects, which include antioxidant, anti-inflammatory and cancer-prevention properties (1, 2). However, full exploitation of its potential benefits has not been realized, owing to poor oral bioavailability and insolubility in aqueous media (3, 4). In 2011, we formulated this naturally occurring polyphenol into nanodisks (ND), conferring water solubility to this compound (5). Formulation of curcumin into ND potentiated its biological effects on cultured hepatoma and lymphoma cells. ND are self assembled bio-nanoparticles comprised of a disk-shaped phospholipid bilayer whose edge is stabilized by a scaffold protein, usually a member of the class of exchangeable apolipoproteins (apo) (6). The apo component imparts tissue targeting potential to the ND platform.

In vitro data indicate curcumin has a pro-apoptotic effect on cultured glioblastoma multiforme (GBM) cells (7-9). Furthermore, intraperitoneal administration of curcumin improved the survival rate of mice with intra-cerebral gliomas (10). Given that GBM cells express increased numbers of heparan sulfate proteoglycans (HSPG) (11) and receptors of the low density lipoprotein (LDL) receptor family (12), we sought to investigate whether ND assembled with apoE would facilitate curcumin delivery to these cells. ApoE is a well known ligand for receptors of the LDL receptor family (13) and binds avidly to HSPGs (14). Results obtained reveal formulation of curcumin ND with apoE as the scaffold component enhances the efficiency with which curcumin is taken up by GBM cells. High resolution confocal fluorescence microscopy images reveal apoE binding to the GBM cell surface together with internalization of curcumin. The finding that the ND scaffold component influences curcumin uptake by GBM cells imply that this biocompatible nanoscale delivery vehicle can be adapted for targeted drug delivery.

3.4. Results

Effect of ND formulation on curcumin uptake by GBM cells

To examine the ability of curcumin-ND to facilitate curcumin uptake by GBM cells, we took advantage of the intrinsic fluorescence of this polyphenol (5). Flow cytometry was used to evaluate curcumin accumulation in cultured SF-767 cells following incubation with free curcumin or curcumin-ND (**Figure 3-1 A**). Cells were incubated with different concentrations of curcumin for 24 h. Untreated cells and cells incubated with empty-ND lacking curcumin gave rise to a single population of cells that served as reference control. Free curcumin induced a concentration dependent shift in cellular fluorescence, indicating uptake of curcumin (**Figure 3-1 B**). Mean cellular curcumin fluorescence intensity was higher for apoA-I curcumin-ND compared to free curcumin although the difference did not reach statistical significance. By contrast, mean cellular curcumin fluorescence intensity increased significantly at all concentrations examined when curcumin was formulated into ND using apoE as scaffold protein. When the same experiment was performed in a second GBM cell line, SF-763, similar results were obtained (**Figure 3-1 C**).

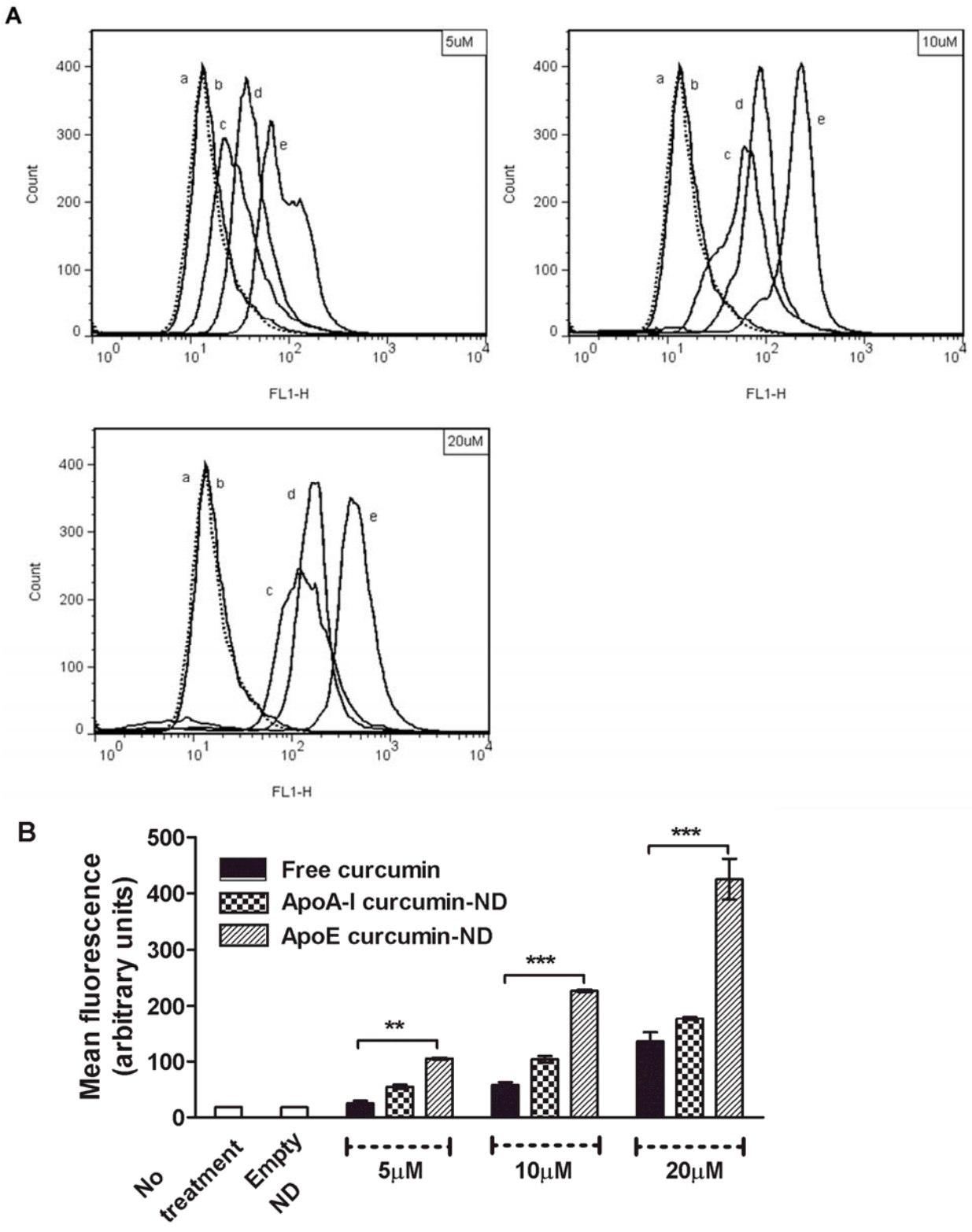
A
5uM
10uM
20uM
Count
FL1-H
a
b
c
d
e
B
Mean fluorescence (arbitrary units)
Free curcumin
ApoA-I curcumin-ND
ApoE curcumin-ND
**
***
***
No treatment
Empty ND
5μM
10μM
20μM

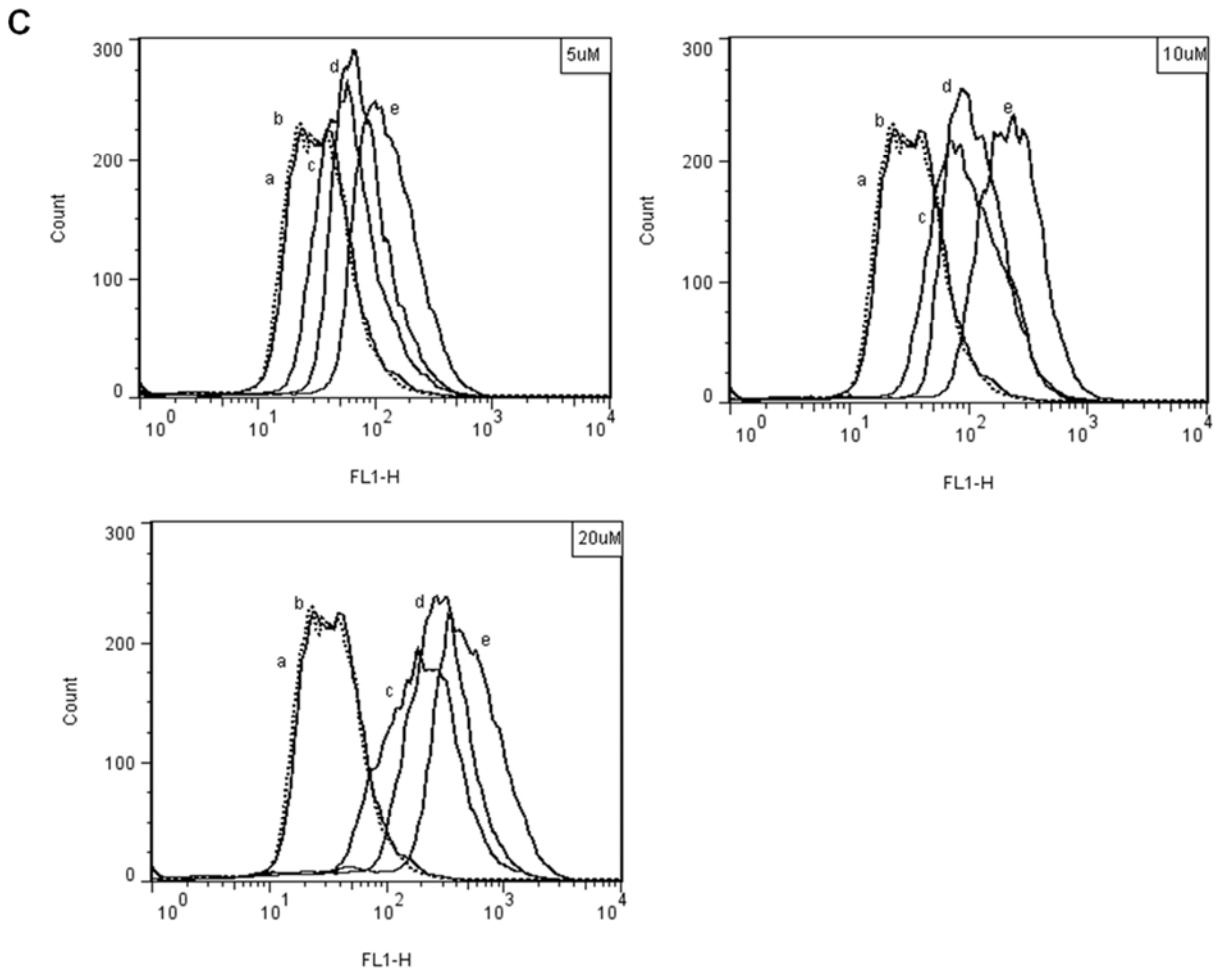

Figure 3-1. ApoE curcumin-ND improves curcumin delivery to GBM cells. Cells were incubated with a) no treatment; b) empty ND; c) free curcumin; d) apoA-I curcumin-ND and e) apoE curcumin-ND. Following incubation, cells were washed and analyzed by flow cytometry. Panel (**A**) shows representative data from three independent experiments performed with SF-767 cells. Each plot represents curcumin fluorescence detected for a cell population after incubation. (**B**) Data shows mean curcumin fluorescence for >95% of the SF-767 cell population as a function of curcumin concentration and formulation. The FL1 channel was used to detect curcumin fluorescence. $^{**}P<0.01$, $^{***}P<0.001$. Panel (**C**) shows overlays of curcumin fluorescence detected in SF-763 cells as a result of different treatments. The three graphs correspond to the three different concentrations tested- 5, 10 and 20 μM. This experiment was repeated one additional time.

Effect of ND formulation on GBM cell viability

SF-767 cells were incubated with free curcumin or curcumin-ND for 48 h followed by determination of cell viability (**Figure 3-2 A**). Compared to free curcumin, apoA-I curcumin-ND showed a greater induction of cell death at 5 and 10 μM curcumin. When GBM cells were incubated with apoE curcumin-ND a significant enhancement in cell death was observed at 5 and 10 μM curcumin, compared to either apoA-I curcumin-ND or free curcumin. Similar results were obtained with SF-763 cells (**Figure 3-2 B**) and are consistent with the increased curcumin fluorescence intensity of cells incubated with apoE curcumin-ND. For SF-767, at 20 μM concentration, all treatment resulted in <25% cell viability. We believe that the 20 μM curcumin concentration might be an overload for a 96-well micro-plate format and hence we were unable to tease out the differences between the formulations at this data point.

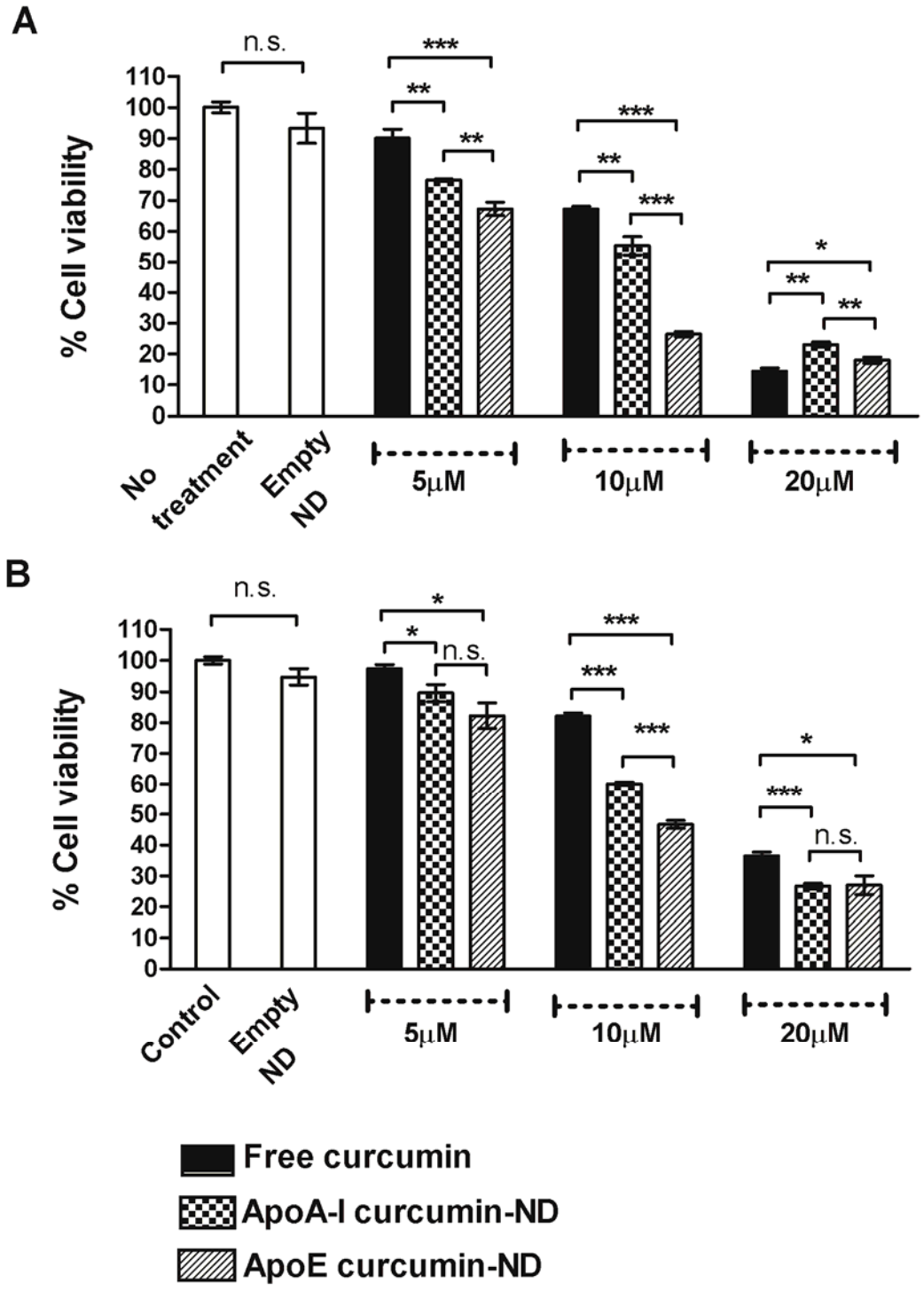

Figure 3-2. Curcumin-ND formulations cause enhanced GBM cell death. (**A**) SF-767 and (**B**) SF-763 cells were incubated with empty ND or the indicated concentrations of free curcumin, apoA-I curcumin-ND and apoE curcumin-ND. After 48 h cell viability was determined using the MTT assay according to the manufacturer's instructions. $^{*}P<0.05$; $^{**}P<0.01$; $^{***}P<0.001$; n.s. = not significant.

Effect of ND formulation on GBM cell apoptosis

The relative ability of free curcumin, apoA-I curcumin-ND and apoE curcumin-ND to induce apoptosis in cultured SF-767 cells was determined (**Figure 3-3**). Compared to untreated cells, empty-ND had no effect on the percentage of apoptotic cells. By contrast, compared to either apoA-I curcumin-ND or free curcumin, apoE curcumin-ND enhanced the percentage of apoptotic cells at all concentrations tested with the difference reaching statistical significance at 10 and 20 μM curcumin.

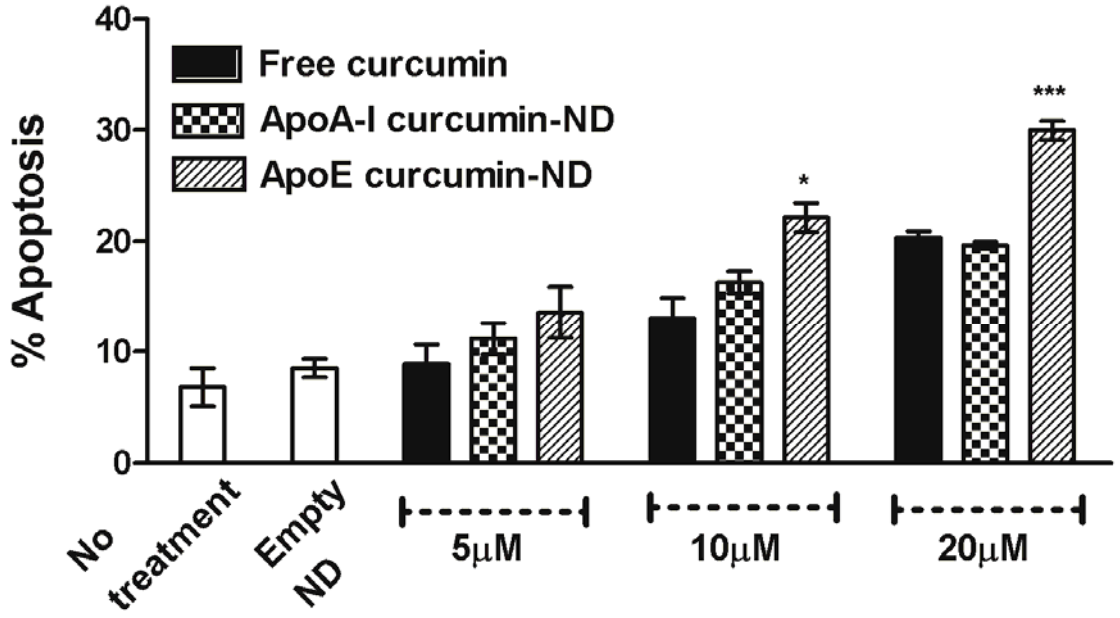

Figure 3-3. ND formulation affects GBM apoptosis. SF-767 cells were incubated with 5, 10 and 20 μM free curcumin, apoA-I curcumin-ND and apoE curcumin-ND. After 40 h the percentage apoptotic cells was assessed by flow cytometry following annexin V and PI staining. Values are the mean ± SD (n=3). *P<0.05; ***P<0.001.

Curcumin uptake follows separation from ND apoE scaffold

To further investigate curcumin uptake by GBM cells following incubation with apoE curcumin-ND, confocal fluorescence microscopy was used to examine the cellular localization of curcumin and apoE (**Figure 3-4**). One h after incubation of SF-767 cells with apoE curcumin-ND, the bulk of the apoE (and presumably the ND particles) was localized at the cell surface. On the other hand, curcumin showed strong intracellular fluorescence intensity. Thus, it appears that apoE curcumin-ND interaction with the surface of GBM cells is followed by curcumin separation from ND and entry to the cell interior with minimal apoE internalization.

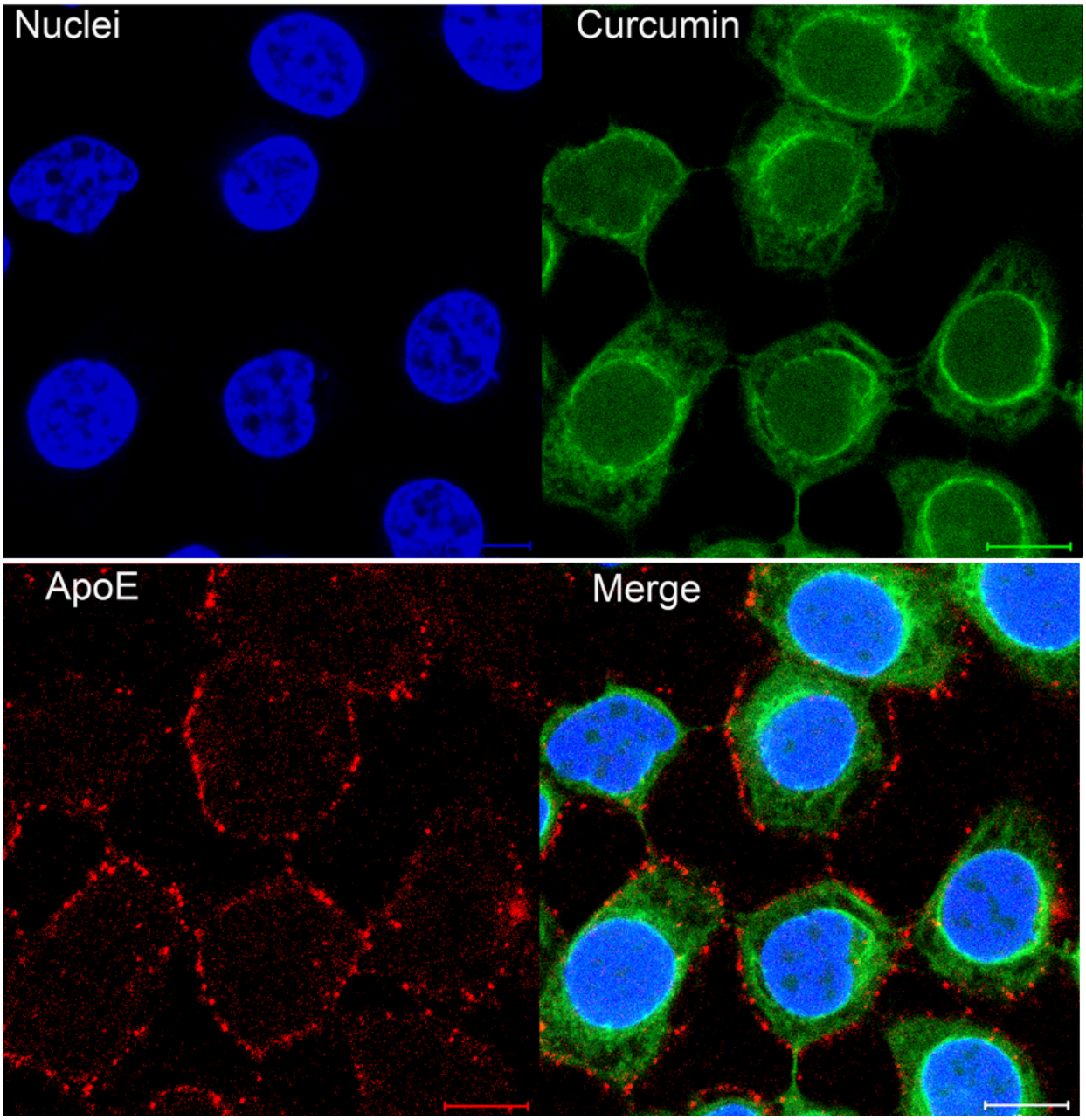

Figure 3-4. Cellular localization of curcumin and apoE. SF-767 cells were incubated with 20 μM apoE curcumin-ND for 1 h at 37 °C and washed to remove unbound ND. Cells were fixed and confocal fluorescence microscopy used to detect curcumin fluorescence. ApoE was detected with mAb 1D7 and a Alexa Fluor 647 labeled anti-mouse secondary antibody. Hoechst 33342 was used to stain the cell nuclei. Scale bar: 10 μm.

Intracellular itinerary of curcumin

To investigate the fate of internalized curcumin as a function of time, confocal microscopy was used to detect curcumin in SF-767 cells (**Figure 3-5 A**). After 30 min incubation with apoE curcumin-ND, curcumin has a diffuse cytosolic distribution. At 1 h, a distinct perinuclear enrichment in curcumin fluorescence appears. After 2 h incubation with apoE curcumin-ND, strong perinuclear fluorescence remained but was complemented by noticeable curcumin fluorescence within the nucleus. At 4 h, the intra-nuclear fluorescence signal was increased and appeared to concentrate at distinct sites. Insofar as others have reported that curcumin can bind DNA's minor groove (15, 16) it is plausible that curcumin localized in the nucleus is associated with chromatin. To explore this, SF-767 cells were treated with apoE curcumin-ND for 24 h and stained with the fluorescent DNA intercalating agent, PI. Confocal images revealed no evidence of overlap between curcumin and PI (**Figure 3-5 B**).

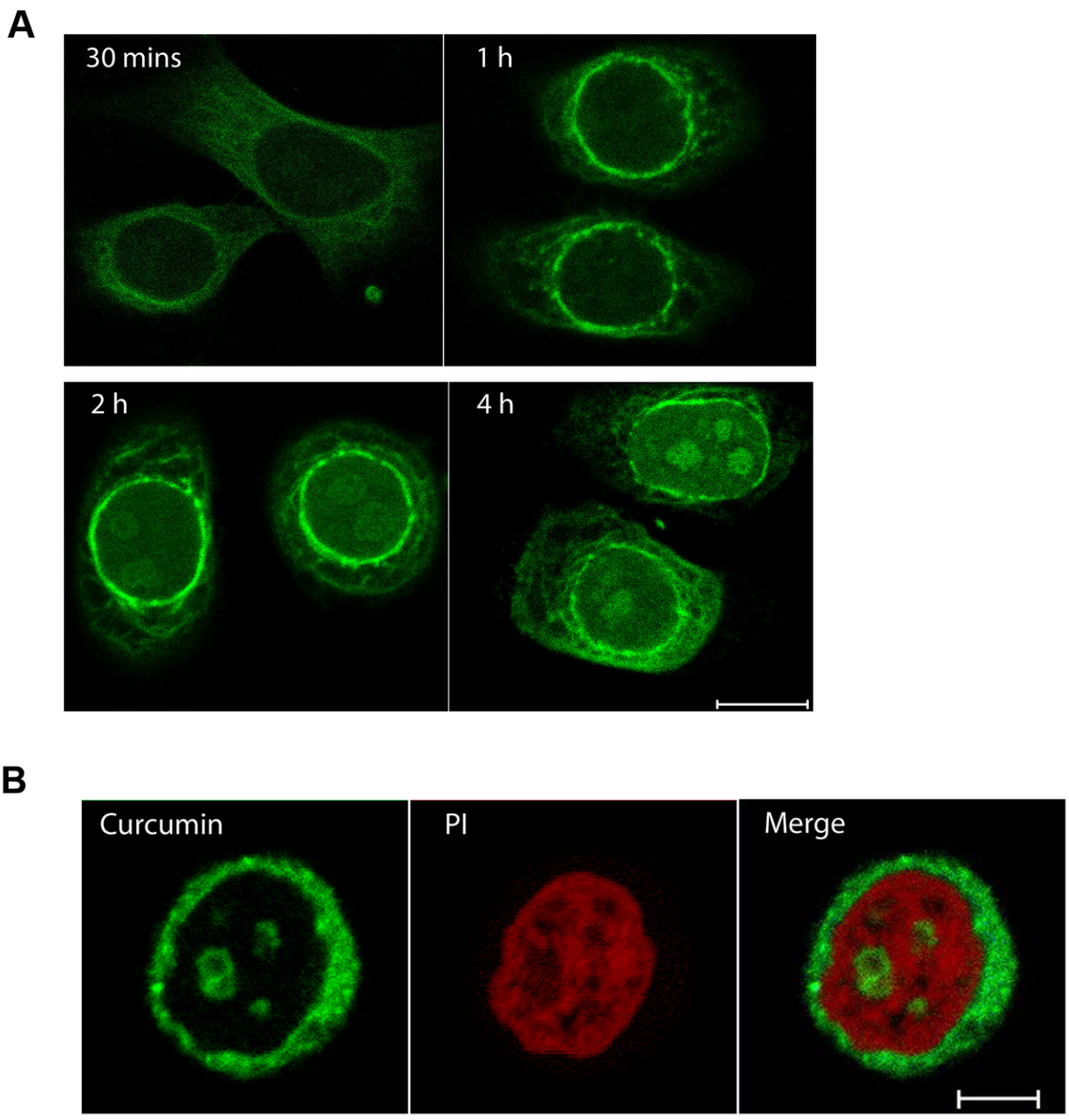

Figure 3-5. Localization of internalized curcumin as a function of time. SF-767 cells were incubated with apoE curcumin-ND (20 μM curcumin) for 30 min, 1, 2 and 4 h and curcumin localization monitored by confocal fluorescence microscopy (**A**). Scale bar: 10 μm. (**B**) Image of a representative SF-767 cell following incubation with apoE curcumin-ND (20 μM curcumin) for 24 h and staining with PI. Scale bar: 5μm.

To confirm that curcumin within the nucleus does not co-localize with PI, Z-stack recording of 0.566 µm thick overlapping images were acquired with a Zeiss LSM710 confocal microscope at 63x magnification (**Figure 3-6 A**). Two-dimensional intensity histogram for the entire Z stack revealed that indeed, at 24 h, curcumin and PI do not co-localize within the nucleus (**Figure 3-6 B**).

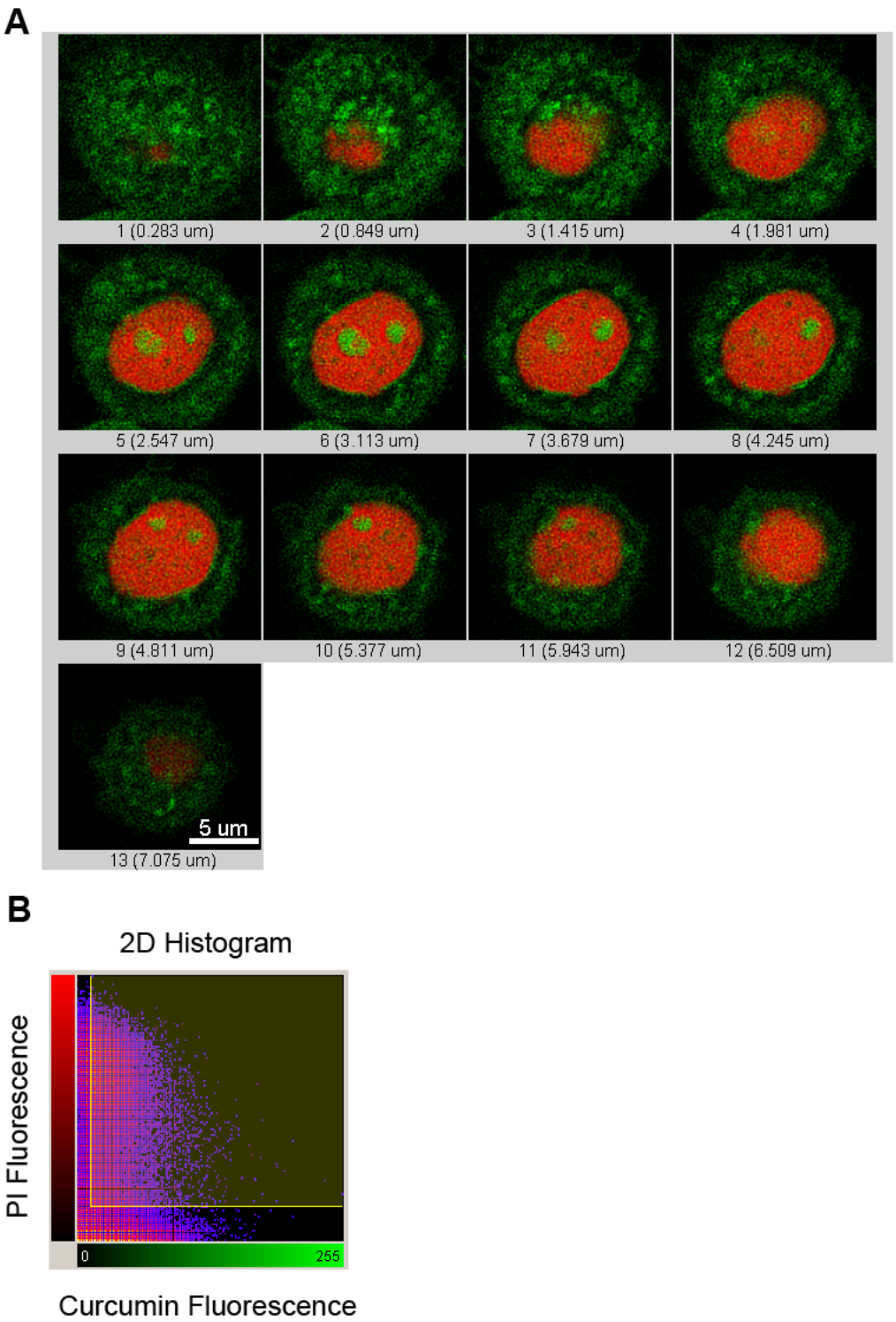

Figure 3-6. PI/curcumin co-localization study. SF-767 cells were incubated with apoE curcumin-ND (20 μM curcumin) for 24 h and co-stained with PI. Images were taken with a Zeiss LSM710 confocal microscope at 63x magnification. (**A**) Z-stack images of a representative cell. The bar in the inset is 5 μm. (**B**) 2D intensity histogram

for the entire Z stack. Data represents pair-wise distribution of voxel intensities obtained from the green (curcumin) and red (PI) channels on a 0 – 255 scale of pixel intensity.

3.5. Discussion

The naturally occurring polyphenol, curcumin, elicits anti-proliferative and pro-apoptotic effects (17). Studies in animal models of GBM revealed that intra-peritoneal injection of curcumin leads to significant reductions in GBM tumor xenograft size and increased time of survival, compared to vehicle-treated controls (9, 10). Whereas these results indicate curcumin has potential therapeutic application against GBM, neither the route of administration nor the vehicle used to administer curcumin are optimal for use in humans. ND are self assembled lipid particles capable of entrapping and solubilizing significant qualities of curcumin. Ease of formulation, intrinsic stability and interchangeability of the ND scaffold protein represent key advantages of this delivery vehicle (18). The fact that formulation of curcumin into ND confers water solubility to this compound, with no loss of biological activity (5, 19), suggests therapeutic benefit may result.

An ideal curcumin delivery vehicle would display tissue targeting capability and facilitate bioactive agent entry to the cell with minimal modification or degradation. In a previous study with curcumin-ND, we showed that curcumin is able to migrate from one ND particle to another, suggesting it does not irreversibly associate with the ND particle (5). In the present study, evidence for controlled release of curcumin from ND was obtained by flow cytometry and confocal fluorescence microscopy. Remarkably, when apoE curcumin-ND were incubated with GBM cells, curcumin was taken up by the cells while nearly all of the apoE scaffold remained localized at the cell surface. Insofar as curcumin uptake by GBM cells was greater when apoE was used as the ND scaffold component, it is conceivable that apoE binding to the GBM cell surface brings curcumin into close cell contact, such that off-loading from the ND particle, and uptake by the cell, is facilitated. It is noteworthy that GBM cells express increased amounts of heparan sulfate proteoglycans (HSPG) (11) and have abundant endocytic receptors of the low density lipoprotein (LDL) receptor family (12). ApoE is well known as a ligand for members of the LDL receptor family (13) and binds avidly to HSPGs (14). Thus, it is conceivable that apoE dependent interaction with one or more of these cell surface components may contribute to the observed enhanced curcumin uptake. While further experiments are required to elucidate the mechanisms involved, the fact that apoE and curcumin do not co-localize within the cell and most apoE remains at the cell surface after nearly all curcumin was internalized, suggests ND whole particle internalization is not involved. Thus, a likely possibility is that apoE promotes ND cell surface interactions, perhaps with HSPGs, facilitating curcumin off-loading and transit to the cell interior, without ND internalization. This proposed mode of delivery may explain the observed perinuclear localization of curcumin one h after incubation of apoE curcumin-ND with GBM cells. Had the entire ND undergone receptor mediated endocytosis, it may be anticipated that curcumin would be directed to the lysosome where degradative enzymes may have an adverse effect on its biological activity. While studying cellular uptake of curcumin as a function of time, we observed an accumulation of curcumin in distinct sites within the nucleus. Following reports that curcumin interacts directly with the minor groove of DNA (15, 16, 20), we performed co-localization studies with PI, a known DNA intercalating agent. Analysis of the deconvolved Z stack merged image

established that the curcumin present in the nucleus of GBM cells did not co-localize with PI. From the results it can be inferred that curcumin does not intercalate DNA. Whereas the nature of the intra-nuclear site of curcumin accumulation is not clear at present, further study of curcumin localization within the nucleus, and correlation with progression toward apoptosis, may provide insight into its mechanism of action.

With regard to biological activity, curcumin is known to induce apoptosis in glioma cells (9, 21). In the present study enhanced uptake of curcumin from apoE ND correlates with enhanced cytotoxic and apoptotic effects suggesting that apoE may be a preferred ND scaffold protein for delivery of curcumin to GBM cells. The apparent off-loading of curcumin from ND in the absence of apoE internalization, combined with the potent biological activity of this formulation, suggests that apoE curcumin-ND may have therapeutic potential. Furthermore, by exploiting the cell binding properties of apoE, or other scaffold protein configurations (22), targeted delivery of curcumin to GBM or other cancer cells *in vivo*, may be possible.

3.6. Methods

Materials

Curcumin was purchased from Cayman Chemical (Ann Arbor, MI) and used without further purification. Dimyristoylphosphatidylcholine (DMPC) was obtained from Avanti Polar Lipids Inc. (Alabaster, AL). The ND scaffold proteins, recombinant human apoA-I and human apoE3 (N-terminal residues 1-183), were expressed in Escherichia coli and isolated as described previously (23, 24). CellTiter 96 Non-Radioactive Cell Proliferation (MTT) Assay kit was obtained from Promega (Madison, WI). Alexa Fluor 647 goat anti-mouse IgG, Hoechst 33342 and the Vybrant Apoptosis Assay Kit were purchased from Life Technologies Corp. (Carlsbad, CA). Monoclonal antibody 1D7, directed against apoE (25) was a gift of Dr. Ross Milne, University of Ottawa.

Curcumin-ND preparation

Curcumin-ND were formulated as described by Ghosh et al. (5). Briefly, 10 mg DMPC was dissolved in chloroform / methanol (3:1 v/v) and dried under a stream of N2 gas. Following dispersal of the prepared lipids in phosphate buffered saline (PBS; 20 mM sodium phosphate, 150 mM sodium chloride, pH 7.0) by bath sonication, 1 mg curcumin (from a 20 mg/ml stock solution in DMSO) was added. Four mg of scaffold protein, either apoA-I or apoE, was added drop-wise with further bath sonication to generate the respective curcumin-ND formulations. ND were then dialyzed (MWCO 6 - 8 kDa) overnight against PBS to remove DMSO, filtered through a 0.22 μm sterile filter and stored at 4 °C until use. Empty-ND, lacking curcumin, were prepared in the same manner except that curcumin was omitted from the formulation.

Quantitation of curcumin incorporation into ND

Curcumin-ND samples were diluted 1:100 in methanol and absorption spectra recorded on a Perkin-Elmer Lambda 20 spectrophotometer. The amount of curcumin incorporated in ND preparations was calculated using a curcumin molar absorption coefficient at 428 nm of 48000 $M^{-1}cm^{-1}$ (26).

Cell culture

The GBM cell lines, SF-763 and SF-767, were obtained from Dr. Trudy M. Forte (Children's Hospital Oakland Research Institute). Cells were maintained in high glucose DMEM (Thermo Scientific Hyclone, South Logan, UT) supplemented with 10% fetal bovine serum, 100 U/ml penicillin and 100 mg/ml streptomycin. Cells were cultured at 37°C in a humidified atmosphere of 5% CO2 and 95% air.

Cell uptake study

A Becton Dickinson FACSCaliber instrument was used to detect curcumin fluorescence inside cells. Cells were plated at 1 x 10^6 cells per well in 6-well plates and allowed to attach overnight. On the following day the culture medium was replaced with reduced serum medium, Opti-MEM (Life Technologies, Carlsbad, CA), supplemented with 5, 10 or 20 μM apoA-I curcumin-ND, apoE curcumin-ND or free curcumin (in DMSO). Untreated cells and cells treated with equivalent amounts of empty-ND served as control. After 24 h the cells were washed with PBS and trypsinized. Cells were centrifuged to remove trypsin and washed with PBS before re-suspending in FACS buffer (PBS with 1% serum and 5 mM EDTA). The mean curcumin fluorescence of >95% of the cell population from the different treatment groups were determined and compared. Values are means ±SD of three independent experiments.

Cell viability assay

Cells were plated in 96-well culture plates at 3000 cells per well and allowed to attach overnight. After 24 h, the medium was replaced with Opti-MEM supplemented with specified concentrations of free curcumin, apoA-I curcumin-ND, apoE curcumin-ND or empty-ND. Forty-eight h after treatment, cell proliferation assays were performed as described by the manufacturer. Briefly, cells were incubated with MTT (3-[4,5-dimethylthiazol-2-yl]-2,5-diphenyltetrazolium bromide) for 2 h at 37°C followed by addition of solubilization buffer (provided by manufacturer). After 1 h incubation at room temperature, absorbance was read at 570 nm. Values expressed are the mean ± S.D. (n = 4) percent cell viability relative to untreated cells.

Apoptosis assay

The Vybrant Apoptosis assay kit was used as per the manufacturer's guidelines to measure cellular apoptosis by flow cytometry. SF-767 GBM cells were plated at a 1 X 10^6 cells/well density on 6-well plates and treated with the specified concentrations of apoA-I or apoE curcumin-ND, free curcumin or empty-ND for 40 h. After treatment, cells were washed with ice-cold PBS, trypsinized, washed an additional time with annexin-binding buffer (kit component) and incubated with Biotin-conjugated annexin V followed by Alexa Fluor 350 streptavidin solution to label early apoptotic cells. One μl of a 1 mg/ml propidium iodide (PI) stock solution was added to each sample prior to flow cytometry measurements on a BD FACSAria.

Confocal fluorescence microscopy

For confocal microscopy, SF-767 cells were plated at 1.5 x 10^5 cells/well, on poly-L-lysine coated 12 mm round coverslips (BD Biosciences, Bedford, MA), in 12-well

plates. After 24 h the medium was replaced with serum-free medium. Cells were incubated with 20 μM curcumin (as apoE curcumin-ND), empty-ND or left untreated. After 1 h, cells were washed with ice-cold PBS and fixed with 4% paraformaldehyde for 10 minutes. Cells were permeabilized with 0.1% Triton (in PBS) followed by incubation with mAb 1D7. For detection, an Alexa Fluor 647 labeled goat anti-mouse IgG secondary antibody was used. Hoechst 33342 was used to stain nuclei. To study the cellular itinerary of curcumin as a function of time, cells were incubated with apoE curcumin-ND for 30 minutes, 1 h, 2 h and 4 h. At each time point, cells were washed with ice-cold PBS and fixed with 4% paraformaldehyde. To investigate curcumin interaction with nucleic acid, cells were incubated with apoE curcumin-ND for 24 h, washed with PBS, fixed with methanol/acetone (1:1 v/v) for 5 minutes and stained with 1 μg/ml PI for 15 minutes. Coverslips were mounted on a glass slide using Vectashield Mounting Medium (Vector Laboratories, Burlingame, CA) and sealed. Confocal images were acquired on a Zeiss LSM710 microscope with a 63X, 1.4NA oil objective with a pinhole of 90 μm. Z-stack recordings of 0.566 μm thick overlapping images were obtained to study PI/curcumin co-localization. Image processing, deconvolution, 3D reconstruction and co-localization analysis were performed with Huygens Essential and Bitplane Imaris Suite package of Scientific Volume Imaging (Hilversum, The Netherlands). The ImarisColoc module was used for co-localization analysis. The module uses an iterative procedure (27) to determine an intensity threshold (in the 0–255 scale of pixel intensity) for each of the two fluorescent labels, green (curcumin) and red (PI). The region of interest (ROI) was defined by using red as the mask channel and the ROI in conjunction with the automatic threshold was used to obtain statistical values for co-localization.

Statistical Analysis

Data from cell proliferation assays are expressed as percent viable cells (viability after treatment with either free curcumin or curcumin-ND over viability after treatment with medium only). Statistical significance between treatment groups was calculated using the two-tailed Student's *t*-test (GraphPad, San Diego, CA). For the apoptosis assay, data are expressed as percent apoptotic cells (annexin V-positive/PI-negative plus annexin V-positive/PI-positive) over total cells. Statistical significance for data obtained from cell uptake study and apoptosis assay were determined by one-way analysis of variance (ANOVA) and Newman-Keuls multiple comparison test. P-values less than 0.05 were considered significant.

3.7. References

(1) Spiller SE, Logsdon NJ, Deckard LA, Sontheimer H. Inhibition of nuclear factor kappa-B signaling reduces growth in medulloblastoma in vivo. BMC Cancer 2011; 11:136.

(2) Epstein J, Sanderson IR, Macdonald TT. Curcumin as a therapeutic agent: the evidence from in vitro, animal and human studies. Br. J. Nutr. 2010; 103:1545-1557.

(3) Anand P, Kunnumakkara AB, Newman RA, Aggarwal BB. Bioavailability of curcumin: problems and promises. Molecular pharmaceutics 2007; 4:807-818.

(4) Schaffer M, Schaffer PM, Zidan J, Bar-Sela G. Curcuma as a functional food in the control of cancer and inflammation. Curr. Opin. Clin. Metab. Care 2011; 6:588-597.

(5) Ghosh M, Singh ATK, Xu W, Sulchek T, Gordon LI, Ryan RO. Curcumin nanodisks: formulation and characterization. Nanomedicine 2011; 7:162-167.

(6) Ryan RO. Bionanotechnology applications of reconstituted high density lipoprotein. J. Nanobiotechnology 2010; 8:28.

(7) Senft C, Polacin M, Priester M, Seifert V, Kögel D, Weissenberger J. The nontoxic natural compound Curcumin exerts anti-proliferative, anti-migratory, and anti-invasive properties against malignant gliomas. BMC Cancer 2010; 10:491.

(8) Huang TY, Tsai TH, Hsu CW, Hsu YC. Curcuminoids suppress the growth and induce apoptosis through caspase-3-dependent pathways in glioblastoma multiforme (GBM) 8401 cells. J. Agric. Food Chem. 2010; 58:10639-10645.

(9) Zanotto-Filho A, Braganhol E, Edelweiss MI, Behr GA, Zanin R, Schröder R, Simões-Pires A, Battastini AM, Moreira JC. The curry spice curcumin selectively inhibits cancer cells growth in vitro and in preclinical model of glioblastoma. J Nutr. Biochem. 2012; 23:591-601.

(10) Perry MC, Demeule M, Regina A, Moumdjian R, Beliveau R. Curcumin inhibits tumor growth and angiogenesis in glioblastoma xenografts. Mol. Nutr. Food Res. 2010; 54:1192-1201.

(11) Steck PA, Moser RP, Bruner JM, Liang L, Freidman AN, Hwang TL, Yung WK. Altered expression and distribution of heparin sulfate proteoglycans in human gliomas. Cancer Res. 1989; 49:2096-2103.

(12) Maletínská L, Blakely EA, Bjornstad KA, Deen DF, Knoff LJ, Forte TM. Human glioblastoma cell lines: levels of low density lipoprotein receptor and low density lipoprotein receptor-related protein. Cancer Res. 2000; 60:2300-2303.

(13) Hauser PS, Narayanaswami V, Ryan RO. Apolipoprotein E: from lipid transport to neurobiology. Prog. Lipid Res. 2011; 50:62-74.

(14) Weisgraber KH, Mahley RW. Human apolipoprotein E: the Alzheimer's disease connection. FASEB J. 1996; 10:1485-1494.

(15) Zsila F, Bikadi Z, Simonyi M. Circular dichroism spectroscopic studies reveal pH dependent binding of curcumin in the minor groove of natural and synthetic nucleic acids. Org. Biomol. Chem. 2004; 2:2902-2910.

(16) Nafisi S, Adelzadeh M, Norouzi Z, Sarbolouki MN. Curcumin binding to DNA and RNA. DNA Cell Biol. 2009; 28:201-208.

(17) Agrawal DK, Mishra PK. Curcumin and its analogues: potential anticancer agents. Med. Res. Rev. 2010; 30:818-860.
(18) Ryan RO. Nanodisks: hydrophobic drug delivery vehicle. Expert Opin. Drug Deliv. 2008; 5:343-351.
(19) Singh ATK, Ghosh M, Forte TM, Ryan RO, Gordon LI. Curcumin nanodisk-induced apoptosis in mantle cell lymphoma. Leukemia and Lymphoma 2011; 52:1537-1543.
(20) Reuter S, Gupta SC, Park B, Goel A, Aggarwal BB. Epigenetic changes induced by curcumin and other natural compounds. Genes Nutr. 2011; 6:93-108.
(21) Kang SK, Cha SH, Jeon HG. Curcumin-induced histone hypoacetylation enhances caspase-3-dependent glioma cell death and neurogenesis of neural progenitor cells. Stem Cells Dev. 2006; 15:165-174.
(22) Iovannisci DM, Beckstead JA, Ryan RO. Targeting nanodisks via an apolipoprotein - single chain variable antibody chimera. Biochem. Biophys. Res. Commun. 2009; 379:466-469.
(23) Ryan RO, Forte TM, Oda MN. Optimized bacterial expression of human apolipoprotein A-I. Protein Expr. Purif. 2003; 27:98-103.
(24) Fisher CA, Wang J, Francis GA, Sykes BD, Kay CM, Ryan RO. Bacterial overexpression, isotope enrichment and NMR analysis of the N-terminal domain of human apolipoprotein E. Biochem. Cell Biol. 1997; 75:45-53.
(25) Weisgraber KH, Rall SC Jr., Mahley RW, Milne RW, Marcel YL, Sparrow JT. Human apolipoprotein E. Determination of the heparin binding sites of apolipoprotein E3. J. Biol. Chem. 1986; 261:2068-2076.
(26) Kunwar A, Barik A, Pandey R, Priyadarsini KI. Transport of liposomal and albumin loaded curcumin to living cells: an absorption and fluorescence spectroscopic study. Biochim. Biophys. Acta. 2006; 1760:1513-1520.
(27) Costes SV, Daelemans D, Cho EH, Dobbin Z, Pavlakis G, Lockett S. Automatic and quantitative measurement of protein-protein colocalization in live cells. Biophys. J. 2004; 86:3993-4003.

CHAPTER 4:

ADAPTING THE NANODISK PLATFORM FOR siRNA DELIVERY

4.1. Abbreviations

AFM = atomic force microscopy
apo = apolipoprotein
DMPC = 1,2-dimyristoyl-*sn*-glycero-3-phosphocholine
DMTAP = 1,2-dimyristoyl-3-trimethylammonium-propane
dsOligo = double stranded oligonucleotide
GAPDH = glyceraldehyde phosphate dehydrogenase
ND = nanodisks
PBS = phosphate buffered saline
RNAi = RNA interference
siRNA = short interfering RNA

4.2. Abstract

RNA interference (RNAi), using short interfering RNA (siRNA), holds enormous therapeutic potential for treating diseases that result from aberrant gene expression. However, a major drawback in the field of siRNA-based therapeutics is the lack of a suitable delivery vehicle for systemic administration of the siRNA molecules. Cationic-lipid nanodisks (ND) were assembled using different ratios of dimyristoylphosphatidylcholine (DMPC), dimyristoyltrimethylaminopropane (DMTAP) and recombinant human apolipoprotein (apo) A-I. Size characterization using atomic force microscopy revealed intact nanometer sized cationic lipid ND were formed at 70:30 DMPC:DMTAP (w/w) ratio. Cationic lipid ND were evaluated for their potential to bind siRNA. Agarose gel retardation assays showed that a synthetic 23-mer double stranded oligonucleotide (dsOligo) bound to cationic lipid ND but not to 100 % DMPC ND. Sucrose density gradient ultracentrifugation studies provided evidence for stable binding of dsOligo to cationic lipid ND and experiments with hepatocarcinoma cells showed that siRNA containing cationic lipid ND efficiently knocked down GAPDH. However, atomic force microscopy of siRNA containing cationic lipid ND provided evidence that the complexes formed were in the μm size range. It is concluded that the increased particle size results from cationic lipid ND stacking as a result of inter-particle electrostatic attraction. Further optimization of cationic lipid ND components should improve their utility for delivery of siRNA cargo.

4.3. Introduction

RNA interference (RNAi) is a natural mechanism of gene regulation conserved in eukaryotes (1). The RNAi pathway is initiated by production of small RNAs that belong to different classes of small regulatory RNAs. Small interfering RNA or siRNA constitute a class of small RNA (2). Most RNAi based therapies employ synthetic siRNAs to silence gene of interest. siRNAs are ~21-23 nucleotide duplexes comprised of perfectly complementary strands. One of the strands, called the guide strand, has perfect sequence homology to target mRNA (3, 4). Once in the cell cytoplasm the siRNA interacts with key proteins assembling a multiprotein-RNA complex called RNA-induced silencing complex or RISC. RISCs use the guide strand of siRNA to cleave target mRNA, thereby preventing translation of disease causing protein. siRNA mediated silencing of validated disease targets have been shown to improve clinical outcome in relevant disease models (5-8). However, siRNA is unstable *in vivo* due to the presence of numerous serum nucleases that cleave the RNA molecules. Moreover, systemic administration of naked siRNA molecules results in their rapid renal clearance. Such challenges have led to the use of chemically modified siRNA molecules (9) and development of both viral (10, 11) and non-viral siRNA delivery strategies. Although viral vectors can effectively deliver expression-based target-complementary short hairpin RNA (shRNA) to induce RNAi *in vivo*, they have been reported to elicit undesirable effects due to endogenous RNAi pathway saturation (12). Non-viral strategies employ peptides (13), aptamers (14), antibody-protamine chimeras (15), cationic lipids (16-18) and cationic polymers (19) as siRNA carriers. Systemic delivery of siRNA encapsulated in cationic lipid-based stable nucleic acid particles (SNALP) (20) and cyclodextrin nanoparticles (21) are the two delivery strategies that are currently under investigation in Phase I/II human clinical trials. Future progress in the field of RNAi-based therapy relies on the development of delivery platforms that are stable, non-immunogenic and allow tissue-specific delivery of siRNA.

Nanodisks (ND) are discoidal ternary complexes comprised of a phospholipid, scaffold protein and an exogenous bioactive agent (22). The scaffold protein (usually a member of the class of amphipathic apolipoproteins) circumscribes the perimeter of a disk shaped phospholipid bilayer, shielding the otherwise exposed fatty acyl chains at the edge of the bilayer (23). Adaptation of ND technology for siRNA delivery is based on the premise that ND can be conferred with a net positive charge via introduction of synthetic cationic lipids. Introduction of a net positive charge is postulated to promote siRNA binding to the ND surface via electrostatic attraction, thereby generating a water soluble vehicle for siRNA transport and delivery (**Figure 4-1**). The zwitterionic dimyristoylphosphatidylcholine (DMPC) and cationic lipid dimyristoyltrimethylammonium propane (DMTAP) were combined with apolipoprotein (apo) A-I to generate cationic lipid ND. Characterization studies provided evidence for siRNA binding and target gene knock down.

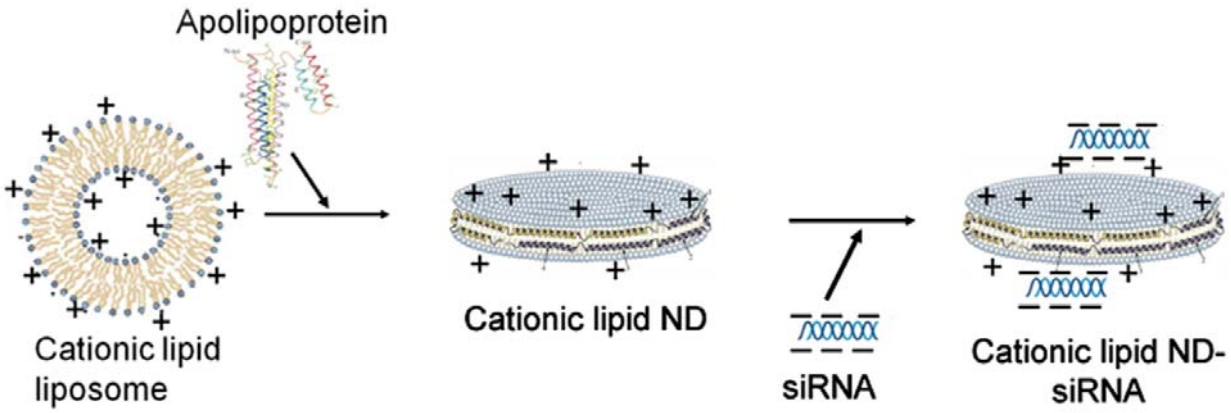

Figure 4-1. Cationic lipid ND formulation scheme. Cationic liposomes are transformed to cationic lipid ND in presence of apolipoprotein. Cationic lipid ND surface charge allows siRNA to bind by electrostatic interaction.

4.4. Results

Cationic lipid ND formation and characterization by AFM

To examine if synthetic cationic lipids can be stably incorporated into ND, two different ratios of DMPC to DMTAP were examined: 70:30 and 50:50 (w/w). In a manner similar to control ND prepared with 100 % DMPC, formulations containing cationic lipid cleared upon addition of apoA-I, indicating complex formation. Upon, storage however, a precipitate formed in the 50:50 DMPC to DMTAP preparation, suggesting these complexes were not stable. Insofar as ND containing 30% cationic lipid remained in solution, subsequent experiments were performed with particles generated using 70:30 ratio of DMPC to DMTAP. Atomic force microscopy revealed that intact cationic lipid ND are in the nanometer size range (**Figure 4-2 A**) with an average height of 4 nm (**Figure 4-2 B** histogram). Based on these results, studies designed to investigate nucleic acid binding were conducted with cationic lipid ND formulated with 30 % DMTAP.

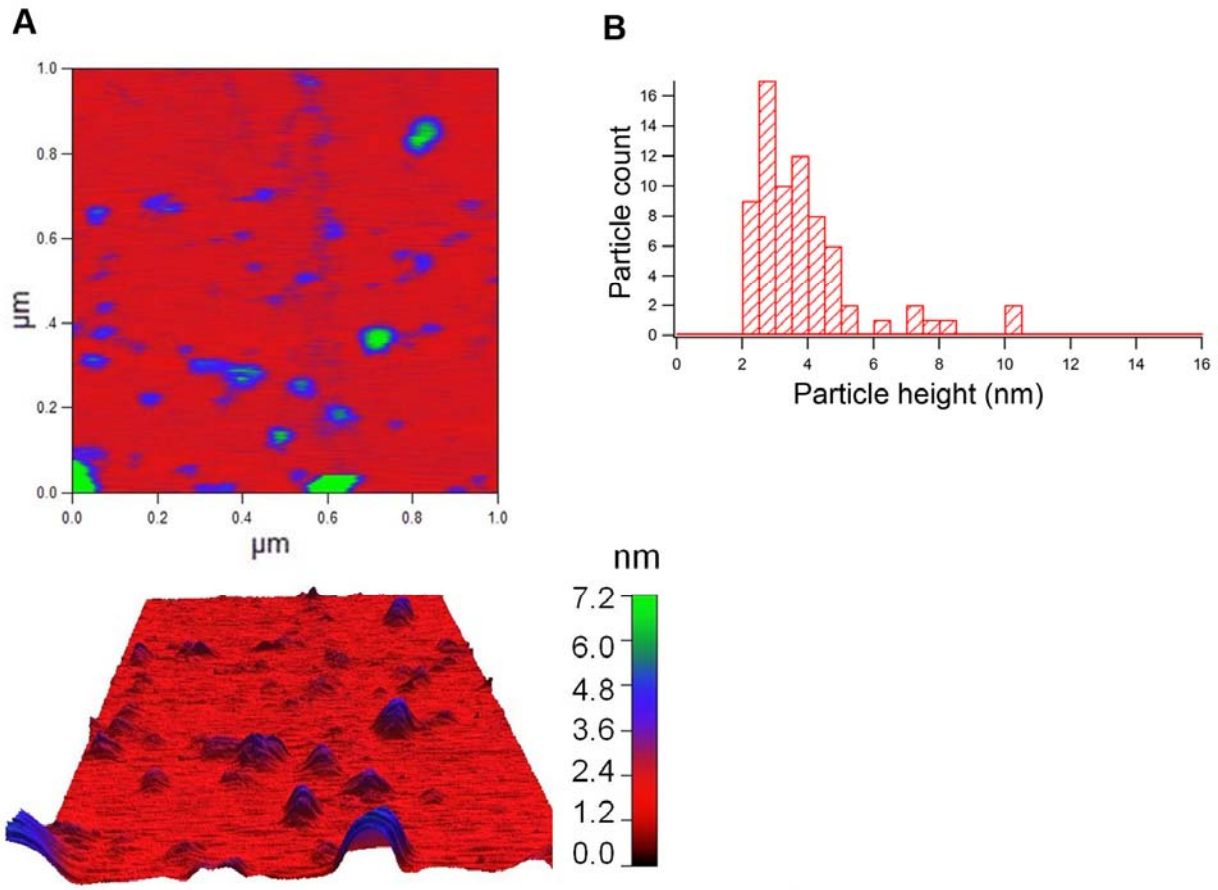

Figure 4-2. Size characterization of cationic lipid ND by AFM. Cationic lipid ND were composed of 70:30 DMPC:DMTAP w/w ratio. Five µl of the sample, at 2 ng/µl protein concentration, was incubated on an atomically flat mica sheet for 5 minutes in PBS and then lightly rinsed. A 1µm x 1µm area was scanned to analyze ND sizes. Panel (**A**) shows raw 2-D (top) and 3-D (bottom) AFM images of cationic lipid ND. The scale included is a color-coded nm scale for particle height. (**B**). Histogram shows heights recorded for the cationic lipid ND. The x-axis shows particle heights and the y-axis represents particle count corresponding to a particular height. Statistics are based on 70 cationic lipid ND particles.

Interaction of nucleic acid with cationic lipid ND

The binding interaction between a model 23 bp dsOligo and cationic lipid ND was studied by altering the ratio of the components. We hypothesized that interaction of dsOligo with cationic lipid ND will neutralize the negative charge character of the dsOligo and, thereby, affect its electrophoretic mobility. In the absence of ND, dsOligo migrates to a characteristic position in the gel (**Figure 4-3**). Furthermore, when dsOligos were incubated with 100% DMPC ND, no change in dsOligo mobility was detected. By contrast, as increasing amounts of cationic lipid ND were incubated with the dsOligo, the intensity of the dsOligo staining band decreased concomitant with the appearance of a new band displaying decreased mobility. At a 1:1 charge ratio of cationic lipid:dsOligo, the dsOligo band was replaced entirely by the slower mobility band. These results indicate that formulation of ND with cationic lipid confers dsOligo binding capability.

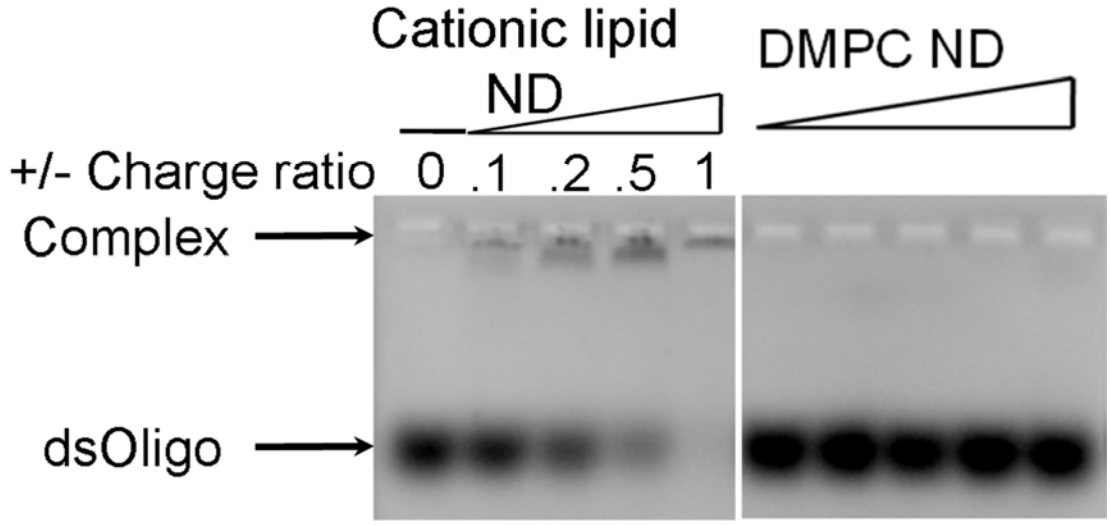

Figure 4-3. Cationic lipid ND form complexes with dsOligo. The pre-formed complexes were analyzed by electrophoresis on an agarose gel (1% w/v) stained with ethidium bromide dye. The cationic lipid ND-dsOligo complexes were formed by incubating increasing amount of cationic lipid ND with a constant amount of dsOligo. The complexes formed correspond to (+/-) charge ratios of 0.1, 0.2, 0.5 and 1. DMPC ND served as control.

Cationic lipid ND-dsOligo complex characterization by sucrose density gradient

Further study revealed that a visible precipitate forms at certain cationic lipid ND:dsOligo ratios but not others. In general, cationic lipid ND-dsOligo complexes formed at ratios close to charge neutralization (i.e. +/- charge ratio of 1) had a greater propensity to develop a precipitate over time. In an effort to define an optimum ratio, complexes formed at different (+/-) charge ratios were subjected to sucrose density gradient ultracentrifugation. Under high-speed ultracentrifugation a particle's sedimentation rate through the gradient is determined by density (24, 25). Following centrifugation, 12 fractions, starting at the top of the gradient, were collected. An aliquot of each fraction was subjected to agarose gel electrophoresis to detect dsOligo while lipid and protein analyses were performed to measure cationic lipid ND components. **Figure 4-4 A** depicts the migration patterns of control cationic lipid ND and dsOligo when centrifuged separately. Whereas cationic lipid ND were recovered predominantly in fractions 4 and 5, the dsOligo was recovered in fractions 2 and 3. Although dsOligos are expected to have a higher density than a cationic lipid ND, the short length of these oligos (23-mer) affects their migration in this system (26).

When cationic lipid ND and dsOligo were pre-incubated at a 1:1 (+/-) charge ratio prior to sucrose gradient ultracentrifugation, a much different migration pattern was observed (**Figure 4-4 B**). In this case, the lipid and protein components of the cationic lipid ND were recovered in gradient fractions 9 - 11. Consistent with formation of a stable complex, dsOligo was also recovered in these fractions. To distinguish between free and cationic lipid ND-bound dsOligo, agarose gel electrophoresis was performed on fractions before and after adding 0.1% Triton X-100. Triton X-100 effectively disrupts cationic lipid ND-dsOligo complexes and releases bound dsOligo such that it can migrate freely in the gel (25, 27). To investigate this further, cationic lipid ND-dsOligo assembled at (+/-) charge ratios of 6, 4, 2, 1 and 0.5 were analyzed (**Figure 4-4 C**). Lower the charge ratio, farther the dsOligo migrated in the sucrose gradient. For cationic lipid ND-dsOligo complexes formed at (+/-) charge ratio 6, the dsOligo molecules were detected in fractions 7 and 8. Complexes with a (+/-) ratio of 4, they migrated to fractions 8 and 9 while complexes with a (+/-) ratio of 2 were recovered in fraction 9. At the lowest (+/-) charge ratios, visible evidence of precipitate formation was observed following centrifugation.

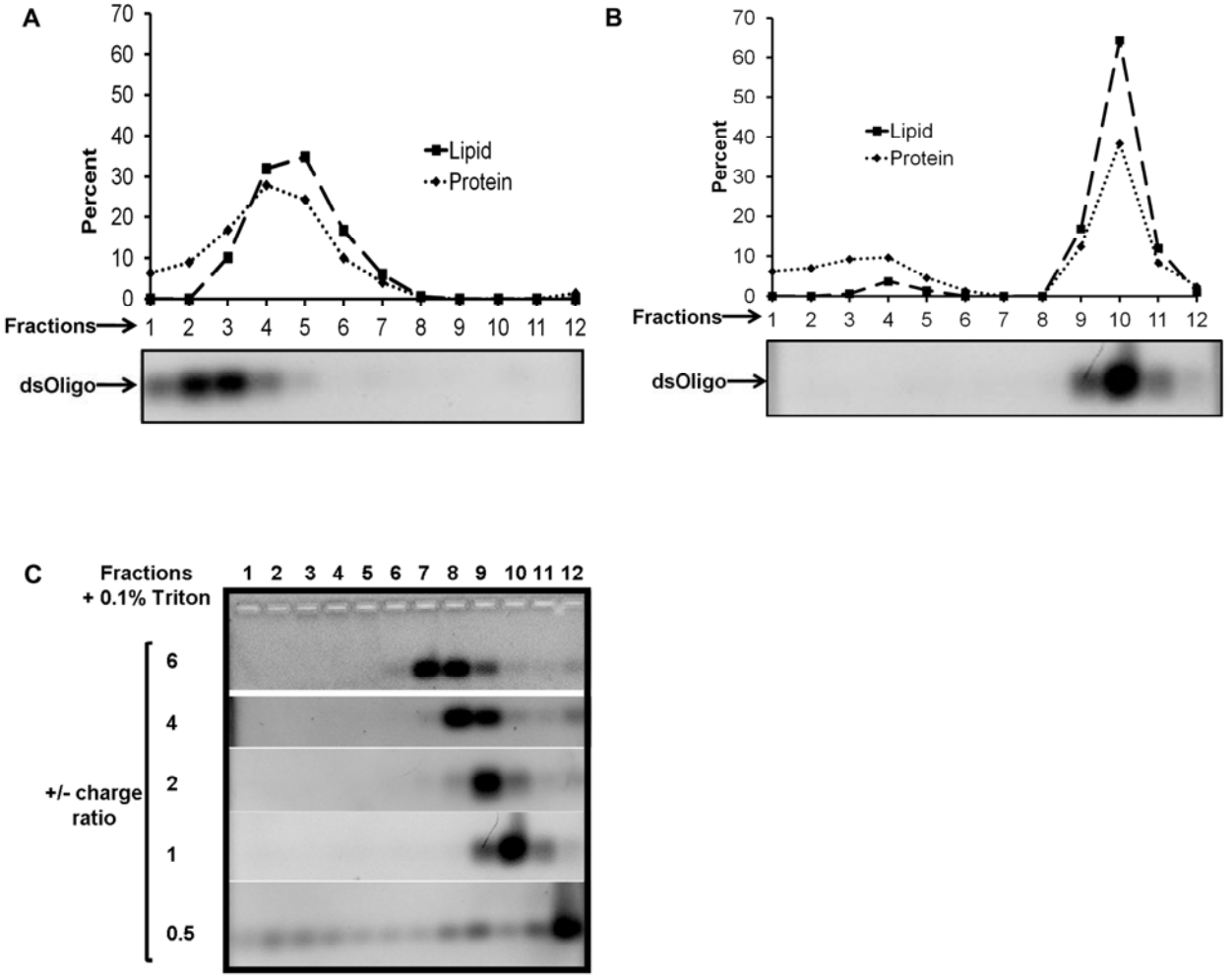

Figure 4-4. Effect of charge ratio on the properties of cationic lipid ND-dsOligo complexes. A 5 to 40% linear sucrose density gradient was prepared and loaded with samples. Samples were centrifuged at 22,000 rpm for 16 h at 10 °C. Twelve fractions, starting from the top of the gradient, were collected. Protein and phospholipid were measured. An aliquot from each fraction was run on a 1% (w/v) agarose gel and stained with ethidium bromide to visualize dsOligo. (**A**). Migration profile for free cationic lipid ND and dsOligo on a linear sucrose density gradient. (**B**). Migration profile for pre-formed cationic lipid ND-dsOligo complexes formed at (+/-) charge ratio of 1. The cationic lipid ND-dsOligo complexes were formed by incubating cationic lipid ND and dsOligo at room temperature for 15 minutes prior to loading on the gradient. (**C**). Migration profiles for dsOligo released from complexes formed at (+/-) charge ratios of 6, 4, 2, 1 and 0.5. The fractions were treated with Triton X-100 to release cationic lipid ND-bound dsOligo. In the absence of Triton X-100 dsOligo did not enter the gel (not shown).

Silencing GAPDH with cationic lipid ND-GAPDH siRNA

A commercially available KDalert™ GAPDH Assay Kit was employed to examine the ability of cationic lipid ND-siRNA complexes to knock down a target gene. The KDalert™ kit contains an optimized GAPDH-specific siRNA and a control siRNA. Cationic lipid ND-siRNA complexes were formed at (+/-) charge ratio of 1. HepG2 cells were treated with cationic lipid ND-GAPDH siRNA, cationic lipid ND-control siRNA, Lipofectamine-GAPDH siRNA (prepared according to manufacturer's protocol) or left untreated for 48 h following which GAPDH enzymatic activity was measured using kit components. Percent remaining GAPDH activity was calculated relative to untreated cells. Cells treated with cationic lipid ND-GAPDH siRNA had 40% remaining GAPDH activity, which translates to a 60% knock down at the protein level (**Figure 4-5**). This result was comparable to knock down levels observed with the commercially available siRNA transfection reagent, Lipofectamine. Cells treated with cationic lipid ND-control siRNA had 100% remaining GAPDH activity (i.e. no knock down).

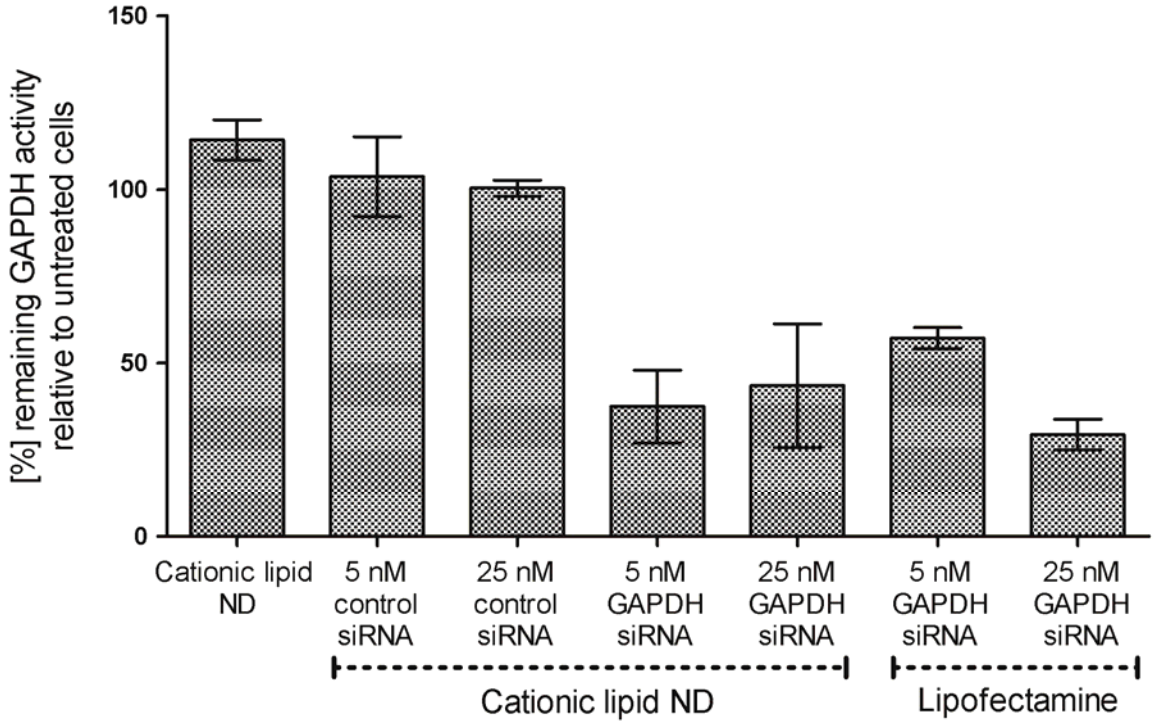

Figure 4-5. Cationic lipid ND-GAPDH siRNA knock down studies. Cationic lipid ND-siRNA were formed at (+/-) charge ratio of 1:1 and Lipofectamine-GAPDH siRNA were formed according to manufacturer guidelines. HepG2 cells were overlaid with pre-formed complexes. KDalert™ GAPDH Assay was performed 48 h after treatment. Percent remaining GAPDH activity is expressed relative to untreated cells. Lipofectamine served as a control delivery reagent. Values are the mean ± SD (n=3).

Characterization of cationic lipid ND-siRNA complexes by AFM

The effect of siRNA binding on cationic lipid ND size and morphology was studied by AFM. GAPDH siRNA was incubated with cationic lipid ND, at 1:1 (+/-) charge ratio, at room temperature followed by AFM analysis. The complexes formed were found to be in the µm size range (**Figure 4-6**).

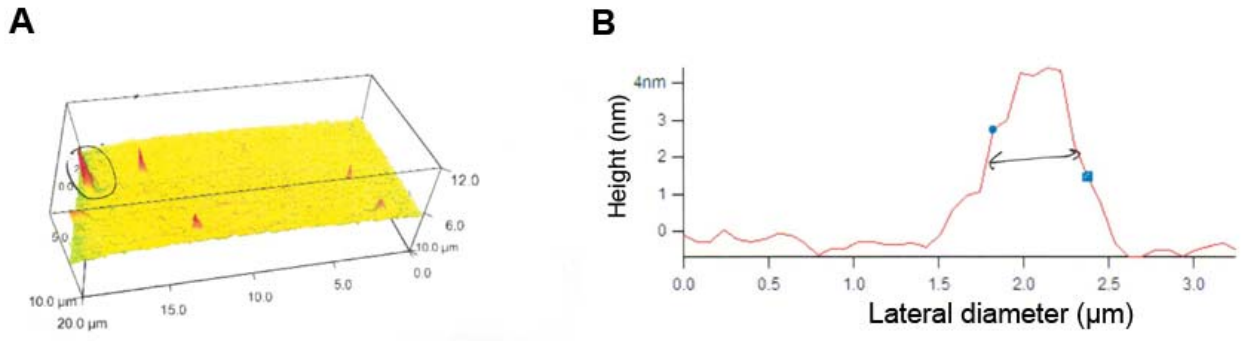

Figure 4-6. Effect of siRNA binding on cationic lipid ND size. Cationic lipid ND were incubated with siRNA at 1:1 (+/-) charge ratio to form cationic lipid ND-siRNA complexes. Size and morphology of the complexes were analyzed by AFM. (**A**). Scanned area showing cationic lipid ND-siRNA complexes as red spikes. The three dimensional window shows x-axis from 0 to 20 µm, y-axis from 0 to 10 µm and z-axis 0 to 12 nm. After scanning a wide field containing multiple particles, the lateral diameter and height of the particles were calculated. (**B**). Lateral diameter and height of a representative cationic lipid ND-siRNA complex (circled in black on panel **A**) is shown. On an average, the lateral diameter of the particles was found to be of µm size range.

4.5. Discussion

In recent years, siRNA-mediated silencing of disease causing genes has emerged as a powerful clinical tool. However, small size, inherent instability and polyanionic nature of the siRNA molecules limit their direct systemic use. Development of a suitable delivery vehicle would protect the siRNA cargo from serum nucleases, prevent the triggering of immune response and facilitate precise intracellular delivery of the siRNA molecules. Cationic lipid ND have the potential to function as a biocompatible siRNA carrier. Our studies show that ND retain their intact nano-sized discoidal morphology with up to 30% DMTAP incorporation. The cationic lipid, DMTAP, confers a positive charge to the ND allowing stable binding with siRNA-like molecules via electrostatic interaction. Evidence of complex formation between cationic lipid ND and siRNA-like dsOligo molecules was obtained from agarose gel retardation assay. Characterization studies using sucrose density gradient revealed stable complex formation between cationic lipid ND and dsOligo. Furthermore, it was noted that the migration of cationic lipid ND-dsOligo complexes in a sucrose density gradient was dependent on the cationic lipid:nucleic acid (+/-) charge ratio. An inverse relationship was observed between the density of complexes and the (+/-) charge ratio at which they were formed. Gene knock down studies were performed in HepG2 cells with complexes formed at 1:1 (+/-) charge ratio. The 60% target gene knock down observed for cationic lipid ND-siRNA complex was found to be comparable to Lipofectamine, a commercially available siRNA delivery reagent. However, atomic force microscopy revealed that the 1:1 (+/-) complexes were μm in size. We hypothesize that the polyanionic siRNA molecules function as a bridge between the cationic lipid ND particles generating larger complexes. Given that these 1:1 complexes migrated to denser fractions of the sucrose density gradient, it is likely that the siRNA molecules also cause compaction of the cationic lipid ND-siRNA complexes. We are currently investigating whether the high knock down observed for the 1:1 complex is a result of passive uptake of these larger, denser complexes. Formulation of smaller complexes, by modifying cationic lipid ND surface charge, with parallel testing of their knock down efficiency is also underway. Cationic lipid ND surface charge can be modified by reducing the amount of DMTAP in ND formulation. Additionally, polyethylene glycol (PEG), which has been shown to confer steric stabilization to complexes (28), can be included in the cationic lipid ND formulation. Inclusion of PEG can be used to cationic lipid ND's advantage since PEG can be couple to molecules like transferrin to impart tissue targeting capability (29).

Studies reported herein demonstrate that cationic lipid ND's ability to deliver siRNA to hepatoma cells in culture with subsequent target gene knock down is comparable to a commercially available siRNA delivery reagent. However, the physical properties of the current formulation might be a limiting factor for its systemic use. Hence, further optimization of the current formulation is underway. Once optimized, the presence of apolipoprotein, as an intrinsic ND component, can be exploited for targeted delivery. Oftentimes, expression of specific receptors is elevated in malignant tissues. Apolipoprotein can be covalently linked to molecules that interact with such receptors. Cationic lipid ND, assembled with the modified apolipoprotein can then be applied for tumor specific delivery of siRNA payload. This strategy is quite feasible since covalent

linkage of proteins to folate followed by receptor mediated uptake of the protein has been reported in literature (30). Moreover, the apolipoprotein can be engineered to act as a ligand for cell surface receptors while retaining its scaffolding function (22, 31). Cationic lipid ND assembled with engineered apolipoprotein would be invaluable for tissue specific delivery of siRNA.

4.6. Methods

Materials

Synthetic lipids DMPC and DMTAP were purchased from Avanti Polar Lipids Inc. (Alabaster, AL). Recombinant apo A-I was expressed in E. coli and isolated as described previously (32). BCA protein assay and the Phospholipids C assay kits were purchased from Thermo Fisher Scientific (Rockford, IL) and Wako Diagnostics (Richmond, VA) respectively. To construct dsOligo, complementary strands 5'-AAC TGG ACT TCC AGA AGA ACA TC-3' and 5'-GAT GTT CTT CTG GAA GTC CAG TT-3' were ordered from Eurofins MWG Operon (Huntsville, AL). Equimolar amounts of the complementary strands were mixed in 1XTE buffer, heated at 95^0C for 5 minutes and then slowly cooled down to room temperature to allow annealing. The KDalert™ GAPDH assay kit and Lipofectamine were from Life Technologies Corp. (Carlsbad, CA).

Cationic lipid ND preparation

Ten mg total lipid, consisting of DMPC and DMTAP in 70:30 weight ratio, was dissolved in chloroform / methanol (3:1 v/v) and dried under a stream of N_2 gas, forming a thin film on a glass vessel wall. Residual organic solvent was removed under vacuum. The prepared lipids were then dispersed in PBS (20 mM sodium phosphate, 150 mM sodium chloride, pH 7.0) by sonication under a N_2 atmosphere. Recombinant apoA-I was added to the solution. Sonication was continued until the turbid mixture became clear, indicating lipid-protein complexes (e.g. cationic lipid ND) had formed. For 10 mg total lipid 4 mg of recombinant protein was added.

Cell culture

HepG2 cells were obtained from American Type Culture Collection. The cells were cultured in minimal essential medium supplemented with 0.1 mM non-essential amino acids, 1 mM sodium pyruvate, and 10% fetal bovine serum at 37°C in a humidified atmosphere of 5% CO_2 and 95% air.

AFM

AFM characterization was carried out on an MFP-3D system (Asylum Research, Santa Barbara, CA). AFM imaging was done in AC mode. For characterization, 5 µl of sample, at 2 ng/µl protein concentration, was incubated on an atomically flat mica sheet for 5 minutes in PBS and then lightly rinsed. A 1µm x 1µm area was scanned to analyze ND sizes. The imaging was performed with the cantilever immersed in PBS.

Agarose gel retardation assay

A synthetic 23-mer dsOligo was incubated for 30 minutes at room temp in PBS with different amounts of cationic lipid ND to form complexes with varying (+/-) charge ratios. The cationic lipid ND-dsOligo complexes were analyzed by electrophoresis on an agarose gel (1% w/v) stained with ethidium bromide dye.

Sucrose density gradient

Cationic lipid ND-dsOligo complexes with varying (+/-) charge ratios were formed by incubating cationic lipid ND and dsOligo at room temperature for 15 minutes. A 5 to 40% linear sucrose density gradient was prepared and pre-formed cationic lipid ND-dsOligo complexes were loaded onto the gradient. Samples were spun down at 22,000 rpm for 16 h at 10^0C on a Beckman L8-80M Ultracentrifuge using a SW41 rotor. Twelve equal fractions, starting from the top of the gradient, were collected from each sample and the fractions were assayed to detect cationic lipid ND components and dsOligo. Protein was quantified by the BCA assay while lipid was measured using the Phospholipids C assay. An aliquot from each fraction was run on a 1% w/v agarose gel, with or without the addition of 0.1% Triton X-100, to detect bound and unbound dsOligo by ethidium bromide staining.

Measurement of GAPDH knock down

The KDalert™ GAPDH kit includes an optimized GAPDH-specific siRNA and a control siRNA. These optimized siRNAs were incubated with cationic lipid ND at 1:1 (+/-) charge ratio for 15 minutes at room temperature. HepG2 cells were seeded on a 24 well plate at a density of 15000 cells/well and allowed to attach overnight. Cells were left untreated or treated with cationic lipid ND-GAPDH siRNA, cationic lipid ND-control siRNA or Lipofectamine-GAPDH siRNA for 48 h. Components provided in the kit were used as per manufacturer's protocol to set up the fluorescent readout of GAPDH enzyme activity remaining after treatment. Briefly, the culture medium was aspirated out from treated cells and cells were lysed with buffer provided in the kit. Twenty µl of the lysate was transferred onto a 96 well plate and immediately after adding 180 µl of master mix with a multichannel pipettor, plate was read on a Wallac VICTOR^2 1420 multilabel counter (Perkin Elmer Life Science) with excitation and emission filters set at 530/590 nm. After 4 minutes a second reading was taken. Increase in fluorescence, obtained by subtracting the initial fluorescence reading from the second reading, was proportional to GAPDH enzyme activity in a sample. Lipofectamine was used as a control siRNA delivery reagent. Treatments were tested in triplicate.

Percent remaining GAPDH activity after treatment with cationic lipid ND-GAPDH siRNA = $(GAPDH_{\text{cationic lipid ND-GAPDH siRNA}} \div GAPDH_{\text{untreated}}) \times 100$

Percent remaining GAPDH activity after treatment with cationic lipid ND-control siRNA = $(GAPDH_{\text{cationic lipid ND-control siRNA}} \div GAPDH_{\text{untreated}}) \times 100$

4.7. References

(1) Li CX, Parker A, Menocal E, Xiang S, Borodyansky L, Fruehauf JH. Delivery of RNA Interference. Cell Cycle 2006; 5:2103-2109.

(2) Jinek M, Doudna JA. A three dimensional view of the molecular machinery of RNA interference. Nature 2009; 457:405-412.

(3) Bernstein E, Caudy AA, Hammond SM, Hannon GJ. Role for a bidentate ribonuclease in the initiation step of RNA interference. Nature 2001; 409:363–366.

(4) Martinez J, Patkaniowska A, Urlaub H, Lu¨ hrmann R, Tuschl T. Single-stranded antisense siRNAs guide target RNA cleavage in RNAi. Cell 2002; 110:563–574.

(5) Frank Y. Xie, Qing Zhou, Ying Liu, Samuel Zalipsky, Xiaodong Yang. Systemic Delivery of Therapeutic siRNA: Opportunities & Challenges. Drug Delivery Technology 2009; 9:32-37.

(6) Hu-Lieskovan S, Heidel JD, Bartlett DW, Davis ME, Triche TJ. Sequence-specific knockdown of EWS-FLI1 by targeted, nonviral delivery of small interfering RNA inhibits tumor growth in murine model of metastatic Ewing's sarcoma. Cancer Research 2005; 65:8984-8992.

(7) Landen CN Jr, Chavez-Reyes A, Bucana C, Schmandt R, Deavers MT, Lopez-Berestein G, Sood AK. Therapeutic *EphA2* gene targeting *in vivo* using neutral liposomal small interfering RNA delivery. Cancer Research 2005; 65:6910-6918.

(8) Zimmermann TS, Lee AC, Akinc A, Bramlage B, Bumcrot D, Fedoruk MN, Harborth J, Heyes JA, Jeffs LB, John M, Judge AD, Lam K, McClintock K, Nechev LV, Palmer LR, Racie T, Röhl I, Seiffert S, Shanmugam S, Sood V, Soutschek J, Toudjarska I, Wheat AJ, Yaworski E, Zedalis W, Koteliansky V, Manoharan M, Vornlocher HP, MacLachlan I. RNAi-mediated gene silencing in non-human primates. Nature 2006; 441:111-114.

(9) De Paula D, Bentley MV, Mahato RI. Hydrophobization and bioconjugation for enhanced siRNA delivery and targeting. RNA 2007; 13:431-456.

(10) McCaffrey AP, Meuse L, Pham TT, Conklin DS, Hannon GJ, Kay MA. RNA interference in adult mice. Nature 2002; 418:38-39.

(11) Zou X, Qiao H, Jiang X, Dong X, Jiang H, Sun X. Downregulation of developmentally regulated endothelial cell locus-1 inhibits the growth of colon cancer. J Biomed. Sci. 2008; 16:33.

(12) Grimm D, Streetz KL, Jopling CL, Storm TA, Pandey K, Davis CR, Marion P, Salazar F, Kay MA. Fatality in mouse due to oversaturation of cellular microRNA/short hairpin RNA pathways. Nature 2006; 441:537-541.

(13) Moschos SA, Williams AE, Lindsay MA. Cell-penetrating-peptide-mediated siRNA lung delivery. Biochem Soc Trans. 2007; 35:807-810.

(14) Fattal E, Bochot A. Ocular delivery of nucleic acids: antisense oligonucleotides, aptamers and siRNA. Adv. Drug Deliv. Rev. 2006; 58:1203-1223.

(15) Song E, Zhu P, Lee SK, Chowdhury D, Kussman S, Dykxhoorn DM, Feng Y, Palliser D, Weiner DB, Shankar P, Marasco WA, Lieberman J. Antibody mediated in vivo delivery of small interfering RNAs via cell-surface receptors. Nature Biotechnology 2005; 23:709-717.

(16) Sørensen DR, Leirdal M, Sioud M. Dag R Sorensen, Marianne Leirdal and Mouldy Sioud. Gene silencing by systemic delivery of synthetic siRNAs in adult mice. J. Mol. Biol. 2003; 327:761-766.
(17) Spagnou S, Miller AD, Keller M. Lipid carriers of siRNA: differences in the formulation, cellular uptake, and delivery with plasmid DNA. Biochemistry 2004; 43:13348-13356.
(18) Morrissey DV, Lockridge JA, Shaw L, Blanchard K, Jensen K, Breen W, Hartsough K, Machemer L, Radka S, Jadhav V, Vaish N, Zinnen S, Vargeese C, Bowman K, Shaffer CS, Jeffs LB, Judge A, MacLachlan I, Polisky B. Potent and persistent in vivo anti-HBV activity of chemically modified siRNAs. Nature Biotechnology 2005; 23:1002-1007.
(19) Urban-Klein B, Werth S, Abuharbeid S, Czubayko F, Aigner A. RNAi mediated gene-targeting through systemic application of polyethylenimine (PEI)-complexed siRNA *in vivo*. Gene Therapy 2005; 12:461-466.
(20) Vaishnaw AK, Cervantes A, Alsina M, Tabernero J, Infante JR, LoRusso P, Shapiro GI, Paz-Ares L, Schwartz G, Weiss G, et al. RNAi in humans: phase I dose-escalation study of ALN-VSP02, a novel RNAi therapeutic for solid tumors with liver involvement. Nucleic Acid Therapeutics 2011; 21, A44.
(21) Davis ME, Zuckerman JE, Choi CH, Seligson D, Tolcher A, Alabi CA, Yen Y, Heidel JD, Ribas A. Evidence of RNAi in humans from systemically administered siRNA via targeted nanoparticles. Nature 2010; 464:1067-1070.
(22) Ryan RO. Nanobiotechnology applications of reconstituted high density lipoprotein. J Nanobiotechnology. 2010; 8:28.
(23) Ryan RO. Nanodisks: hydrophobic drug delivery vehicles. Expert Opinion Drug Delivery 2008; 5:343-351.
(24) Xu Y, Hui SW, Frederik P, Szoka FC Jr. Physicochemical characterization and purification of cationic lipoplexes. Biophysical Journal 1999; 77:341-353.
(25) Wheeler JJ, Palmer L, Ossanlou M, MacLachlan I, Graham RW, Zhang YP, Hope MJ, Scherrer P, Cullis PR. Stabilized plasmid-lipid particles: construction and characterization. Gene Therapy 1999; 6:271-281.
(26) Djikeng A, Shi H, Tschudi C, Shen S, Ullu E. An siRNA ribonucleoprotein is found associated with polyribosomes in Trypanosoma brucei. RNA 2003; 9:802-808.
(27) Auguste DT, Furman K, Wong A, Fuller J, Armes SP, Deming TJ, Langer R. Triggered release of siRNA from poly(ethylene glycol)- protected, pH-dependent liposomes. J. Control Release 2008; 130:266-274.
(28) Needham D, McIntosh TJ, Lasic DD. Repulsive interactions and mechanical stability of polymer-grafted lipid membranes. Biochim Biophys Acta 1992; 1108:40-48.
(29) Ishida O, Maruyama K, Tanahashi H, Iwatsuru M, Sasaki K, Eriguchi M, Yanagie H. Liposomes bearing polyethyleneglycol-coupled transferrin with intracellular targeting property to the solid tumors in vivo. Pharm Res 2001; 18:1042-1048.
(30) Leamon CP, Low PS. Christopher P. Delivery of macromolecules into living cells: A method that exploits folate receptor endocytosis. PNAS 1991; 88:5572-5576.
(31) Iovannisci DM, Beckstead JA, Ryan RO. Targeting nanodisks via a single chain variable antibody--apolipoprotein chimera. Biochem Biophys Res Commun. 2009; 379:466-469.

(32) Ryan RO, Forte TM, Oda MN. Optimized bacterial expression of human apolipoprotein A-I. Protein Expr Purif 2003; 27:98-103.

CHAPTER 5:
CONCLUDING REMARKS

Summary and future directions

Several drugs that are either in the clinic or undergoing clinical evaluation would benefit from the development of an efficient delivery modality. Nanodisks (ND), comprised of a tripartite system of lipid, apolipoprotein (apo) and a bioactive agent, represent a simple straightforward platform that can be modified at the molecular level depending on specific delivery needs. Components of ND can be varied individually or in tandem to suit the formulation for cell type specific delivery of different biomolecules. The basic phospholipid-apolipoprotein composition is well-suited for hydrophobic bioactive compounds such as curcumin. Inclusion of an optimum mole percent of cationic lipid in the phospholipid bilayer allows ND to function as a carrier for small interfering RNA (siRNA) molecules, a novel class of macromolecule with therapeutic potential.

The nano-scale dimension and the discoidal morphology of ND loaded with curcumin were confirmed by high resolution atomic force microscopy. Incorporation of curcumin into ND rendered water solubility to the polyphenol. Compared to free curcumin, curcumin-ND mediated more efficient cellular uptake of curcumin resulting in potent biological effects in different mammalian tumor cell lines. Although the scaffold can mediate interaction between ND and cell surface proteins, the effects of such interaction on cargo delivery had not been evaluated before. ApoE is a known ligand for heparan sulfate proteoglycans (HSPG) and receptors of the low-density receptor family. Glioblastoma multiforme, an aggressive type of primary brain tumor, characterized by high expression of such receptors presented a good model to test the effects of ND scaffold-cell surface interaction on curcumin delivery. Indeed, in the glioblastoma cells, apoE scaffold-dependent higher intracellular accumulation of curcumin was observed. Moreover, compared to apoA-I curcumin-ND, apoE curcumin-ND mediated more potent anti-proliferative and apoptotic effects. High resolution confocal microscopy provided evidence of apoE binding to the glioma cell surface. Thus it is possible that apoE binding to cell surface receptors brings curcumin in close proximity to these cells which, in turn, mediates enhanced cellular uptake of the curcumin cargo. Future experiments will be directed towards confirming that the enhanced curcumin uptake observed resulted directly from interaction between apoE ND scaffold and proteins on glioma cell surface. To this end heparin, a molecule that blocks apoE binding to HSPGs, will be used. Comparison of curcumin uptake in cells treated with apoE curcumin-ND, either in the presence or absence of heparin, would confirm whether the improved cargo off-loading is due to the specific interaction between apoE and HSPGs on glioma cells. Taking advantage of curcumin's intrinsic fluorescence, I have set up a cell-based flow cytometry assay to detect and quantitate intracellular curcumin. This straightforward and inexpensive assay can be used as a tool to conduct the above-mentioned mechanistic study. This assay can also be used to study ND's efficiency to deliver curcumin to cultured cells in the presence of increasing amounts of serum. Such experiments are necessary prior to setting up *in vivo* efficacy studies with curcumin-ND in animal models.

Substituting thirty percent of ND's DMPC content with the cationic lipid, dimyristoyltrimethylammonium propane (DMTAP), generated intact nano-particles that stably bound to siRNA-like deoxyribonucleotide molecules. In cultured hepatoma cells cationic lipid ND-bound GAPDH siRNA caused efficient target gene knock down. However, atomic force microscopy revealed that siRNA binding to cationic lipid ND significantly increases the size of complexes formed. Such large complexes might not be suitable for *in vivo* applications. Thus future efforts will be directed towards modifying cationic lipid ND surface charge to prevent self association in the presence of siRNA. Reducing the current DMTAP content and inclusion of polyethylene glycol, on cationic lipid ND-siRNA complex size, are some of the strategies under investigation. Further optimization of the current cationic lipid ND composition will yield a superior siRNA nano-carrier.

ND are self assembled nanobioparticles that can be tuned at the molecular level for targeted drug delivery. With further tissue targeting capabilities via scaffold protein engineering, the future for ND as a drug delivery vehicle looks bright.